Thermal Misalignment of Scalar Dark Matter

Brian Batell
University of Pittsburgh
with Akshay Ghalsasi, arXiv:2109.04476

2022 CAU BSM Workshop
February 10, 2022

Dark Matter

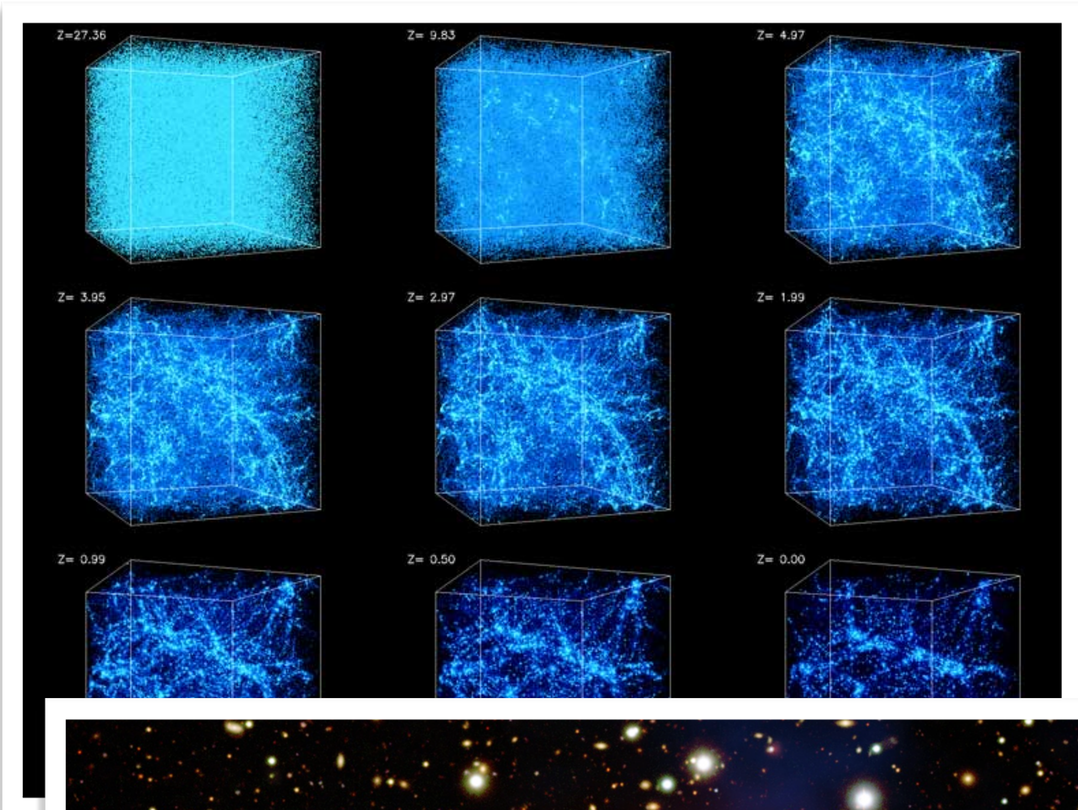

Z=27.36
Z= 9.83
Z= 4.97
Z= 3.95
Z= 2.97
Z= 1.99
Z= 0.99
Z= 0.50
Z= 0.00

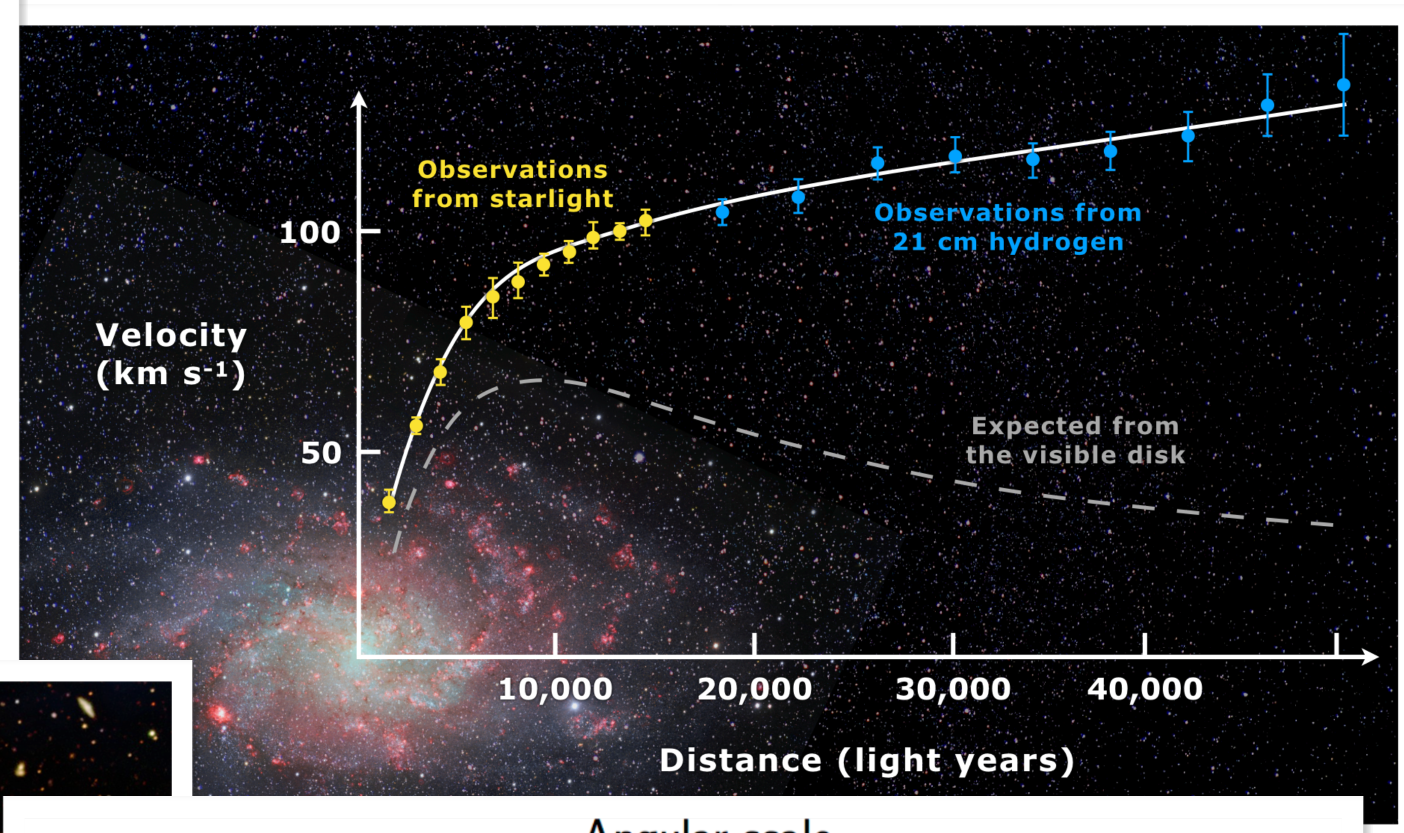

Observations from starlight
Observations from 21 cm hydrogen
Velocity (km s-1)
100
50
Expected from the visible disk
10,000
20,000
30,000
40,000
Distance (light years)

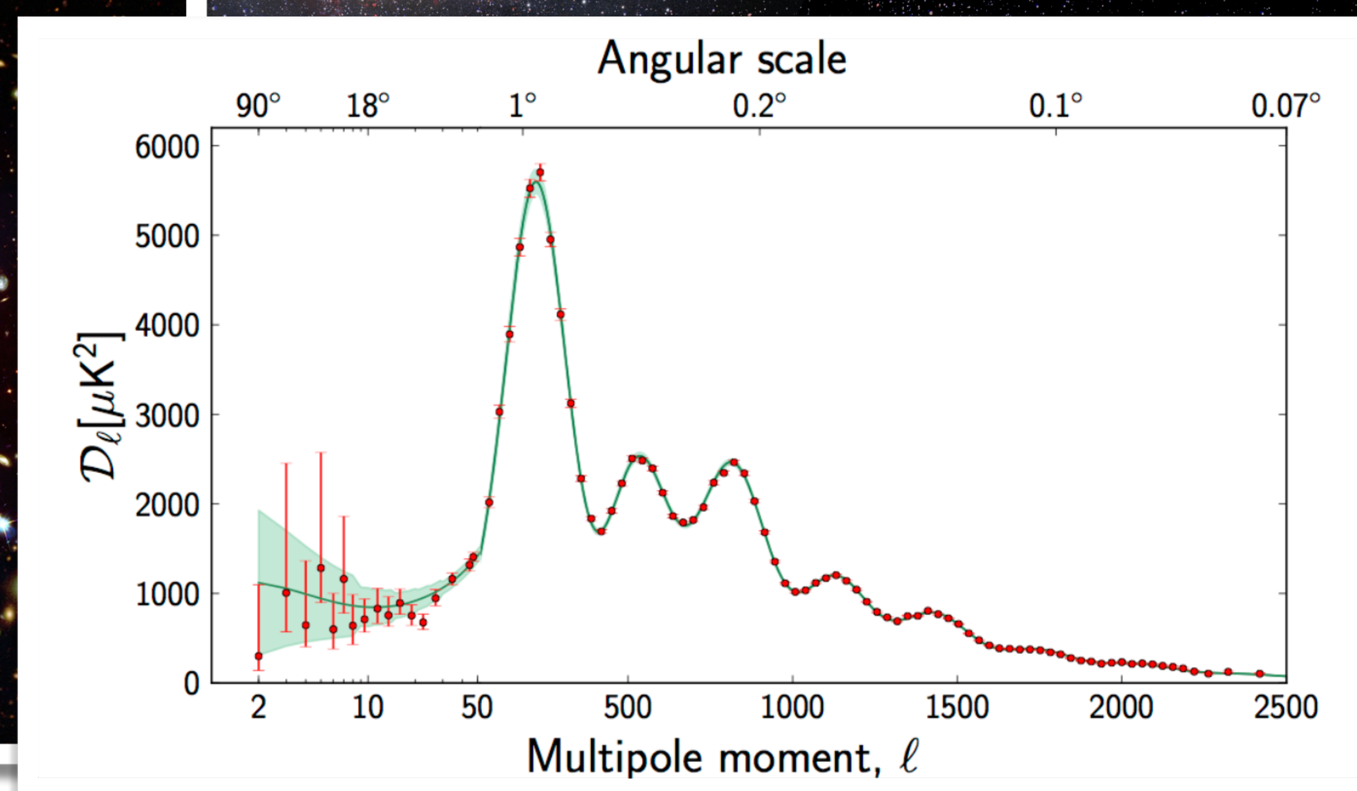

Angular scale
90°
18°
1°
0.2°
0.1°
0.07°
6000
5000
4000
3000
2000
1000
0
$\mathcal{D}_\ell [\mu K^2]$
2
10
50
500
1000
1500
2000
2500
Multipole moment, ℓ

Dark Matter

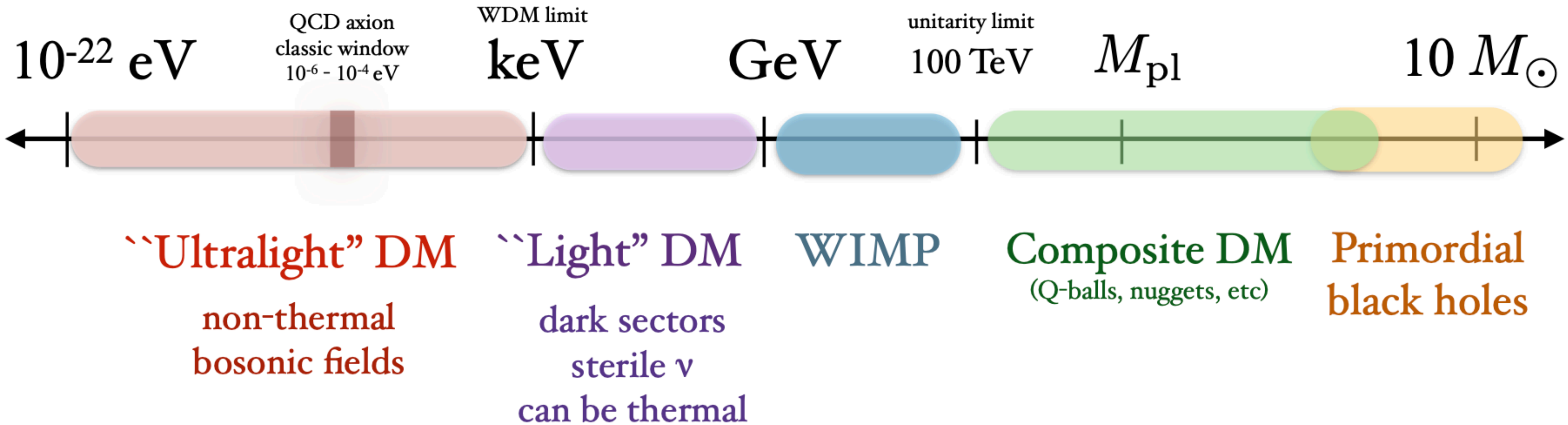

Fig. from T. Lin, TASI Lectures

Dark Matter

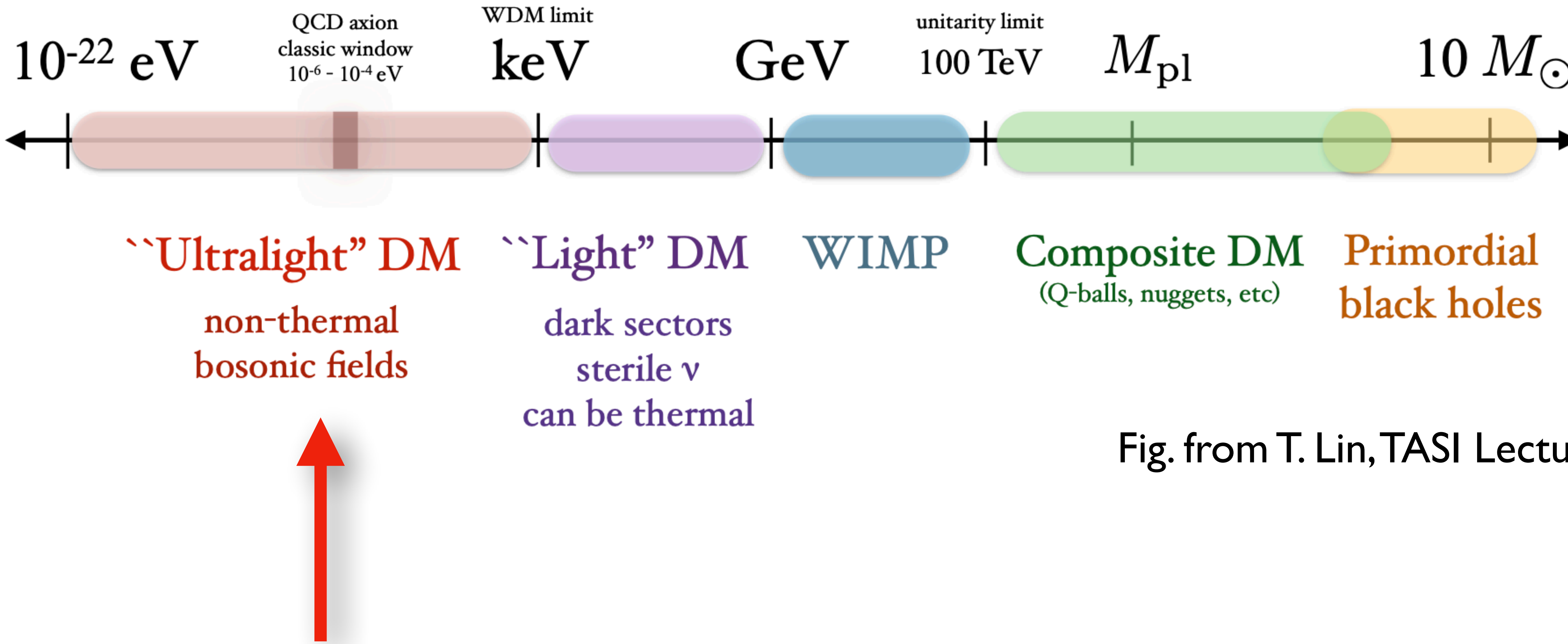

Fig. from T. Lin, TASI Lectures

My focus today

Motivation and Plan

- The misalignment mechanism is a generic dark matter production mechanism for such ultralight dark matter
  - Sensitivity to initial conditions?
  - Connection with short distance particle physics parameters?

- I will describe a new mechanism — *thermal misalignment* — to dynamically generate large misalignment from generic initial conditions.

- The mechanism relies on a coupling of the scalar dark matter to a fermion in thermal equilibrium and the resulting finite temperature potential

- The phenomenology of a realistic scenario where DM couples to the muon will be discussed

See also talk by Eung Jin Chun for related ideas

The classic misalignment mechanism

- Consider the dynamics of massive scalar field ϕ in the early universe
- Starting from some initial scalar field value ϕ_i at early times the scalar evolves according to the equation of motion:

[Preskill, Wise, Wilczek; Abbott, Sikivie; Dine, Fischler, '83]

$$\ddot{\phi} + 3H\dot{\phi} + m_\phi^2 \phi = 0$$

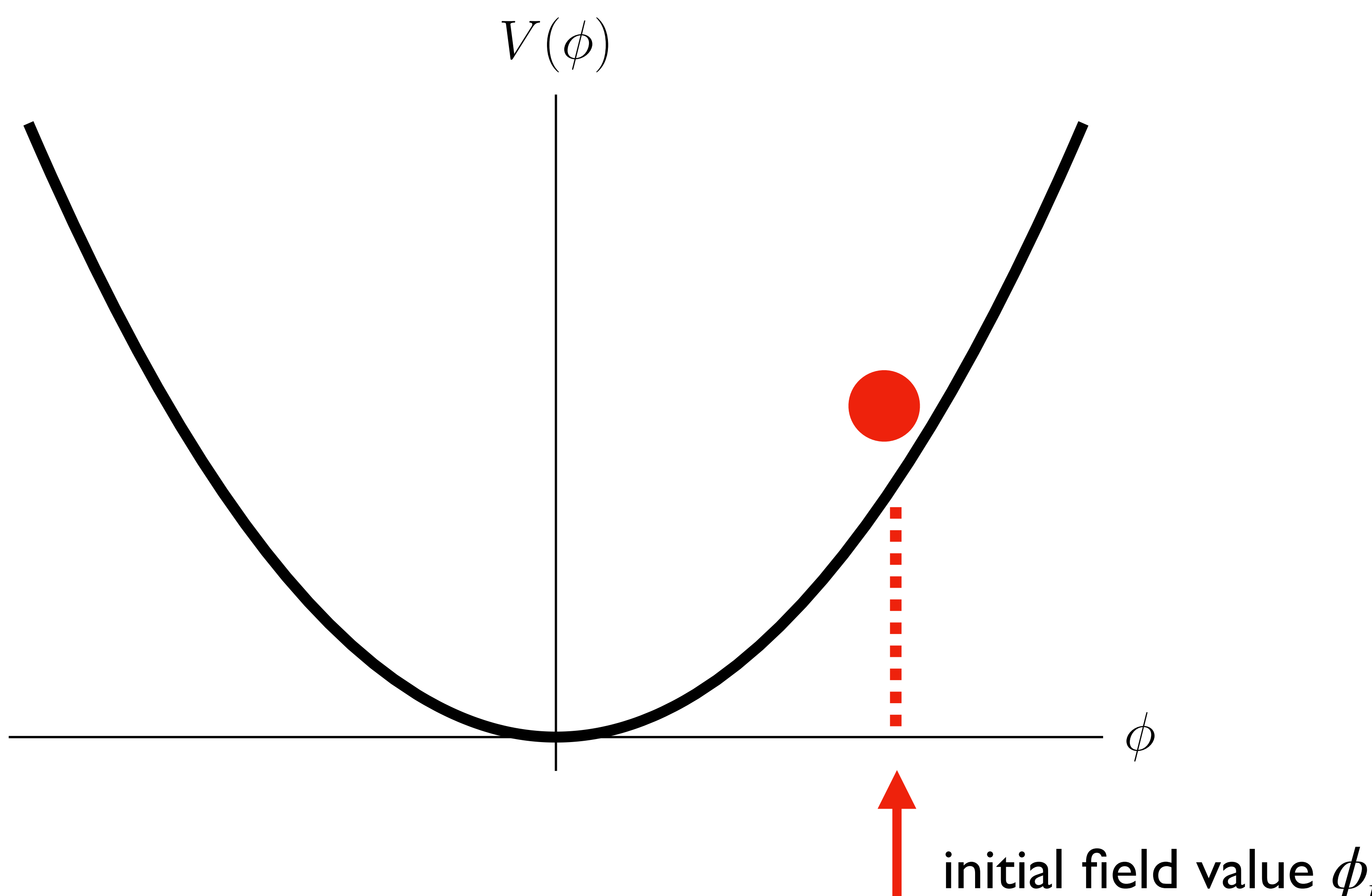

The classic misalignment mechanism

- At early times (high temperature) the scalar is held up by Hubble friction and remains approximately at its initial field value.

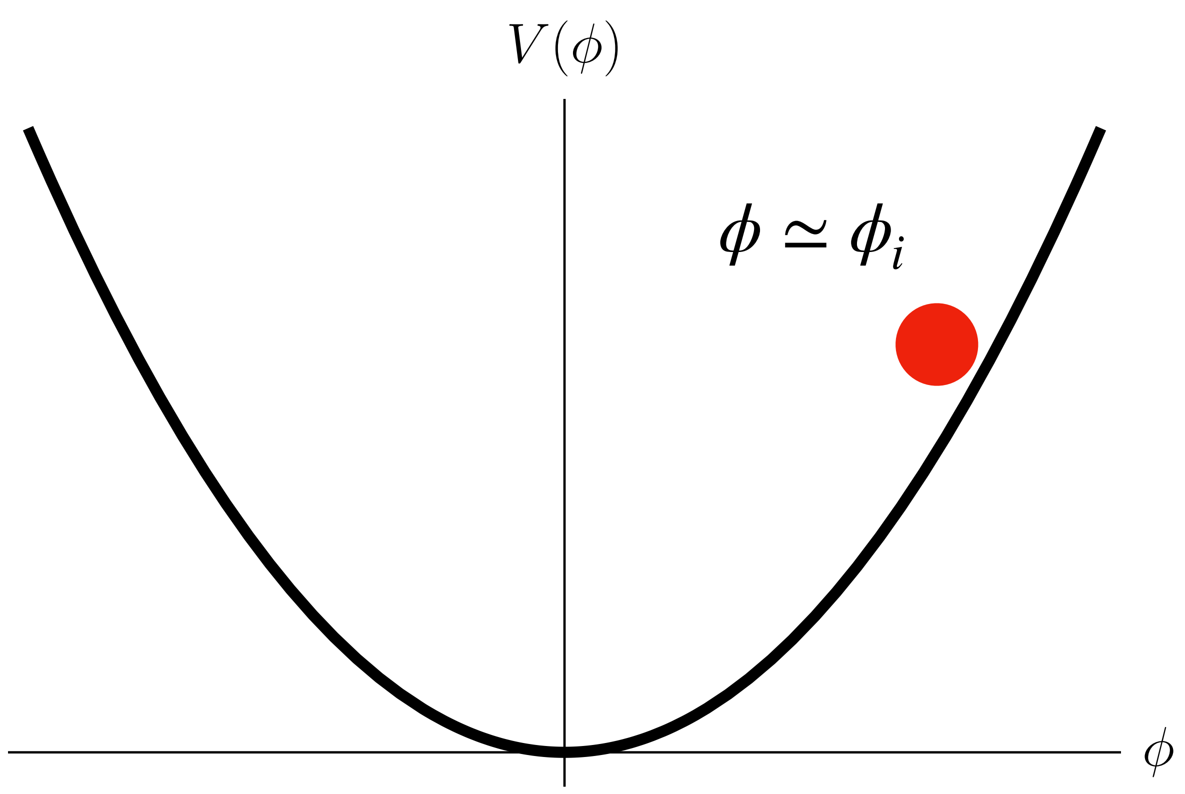

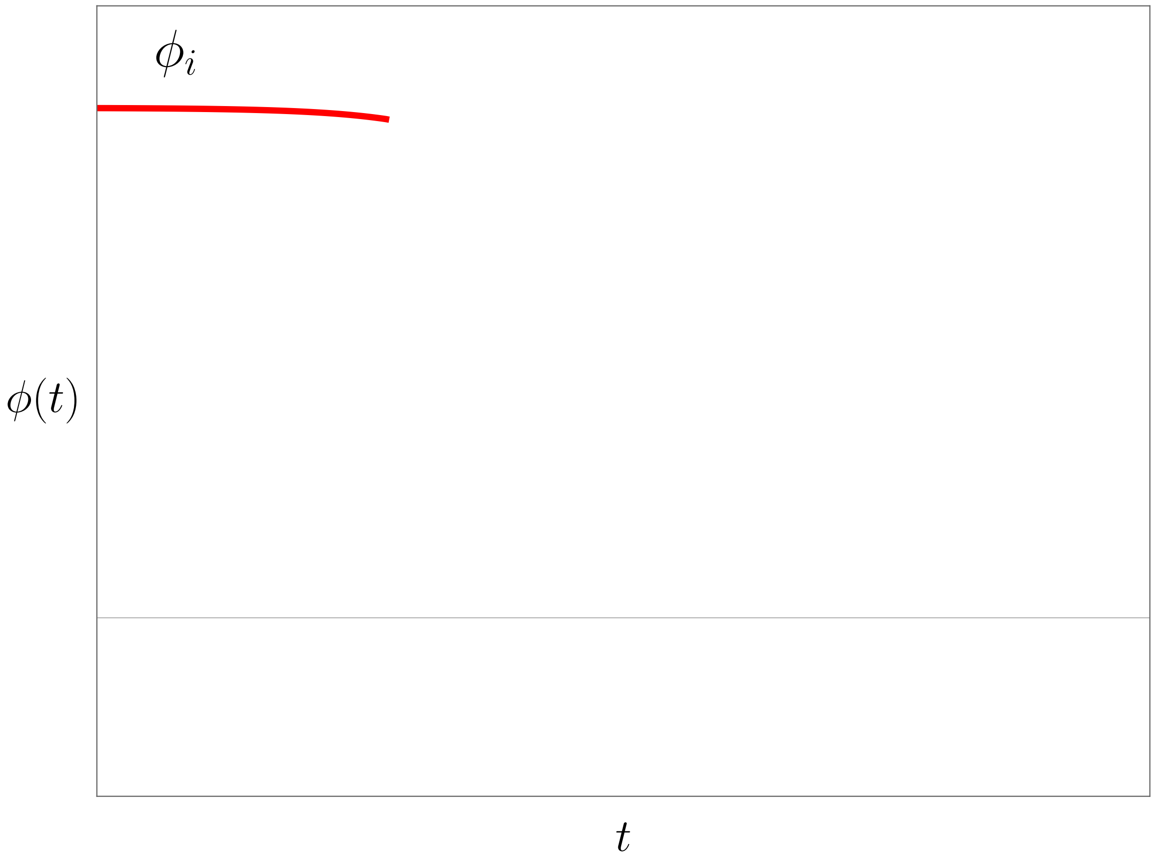

The classic misalignment mechanism

- At early times (high temperature) the scalar is held up by Hubble friction and remains approximately at its initial field value.
- As the universe cools, the Hubble eventually drops below the scalar mass. This signals the onset of scalar oscillations.

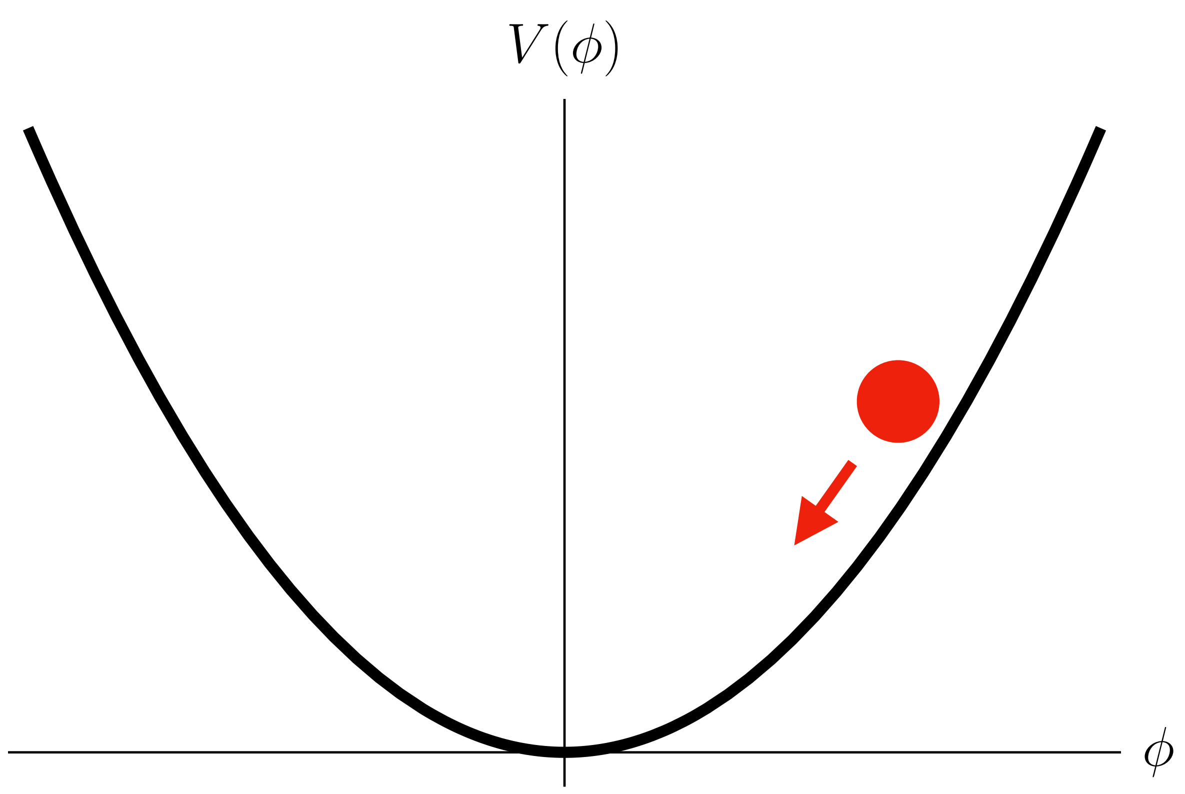

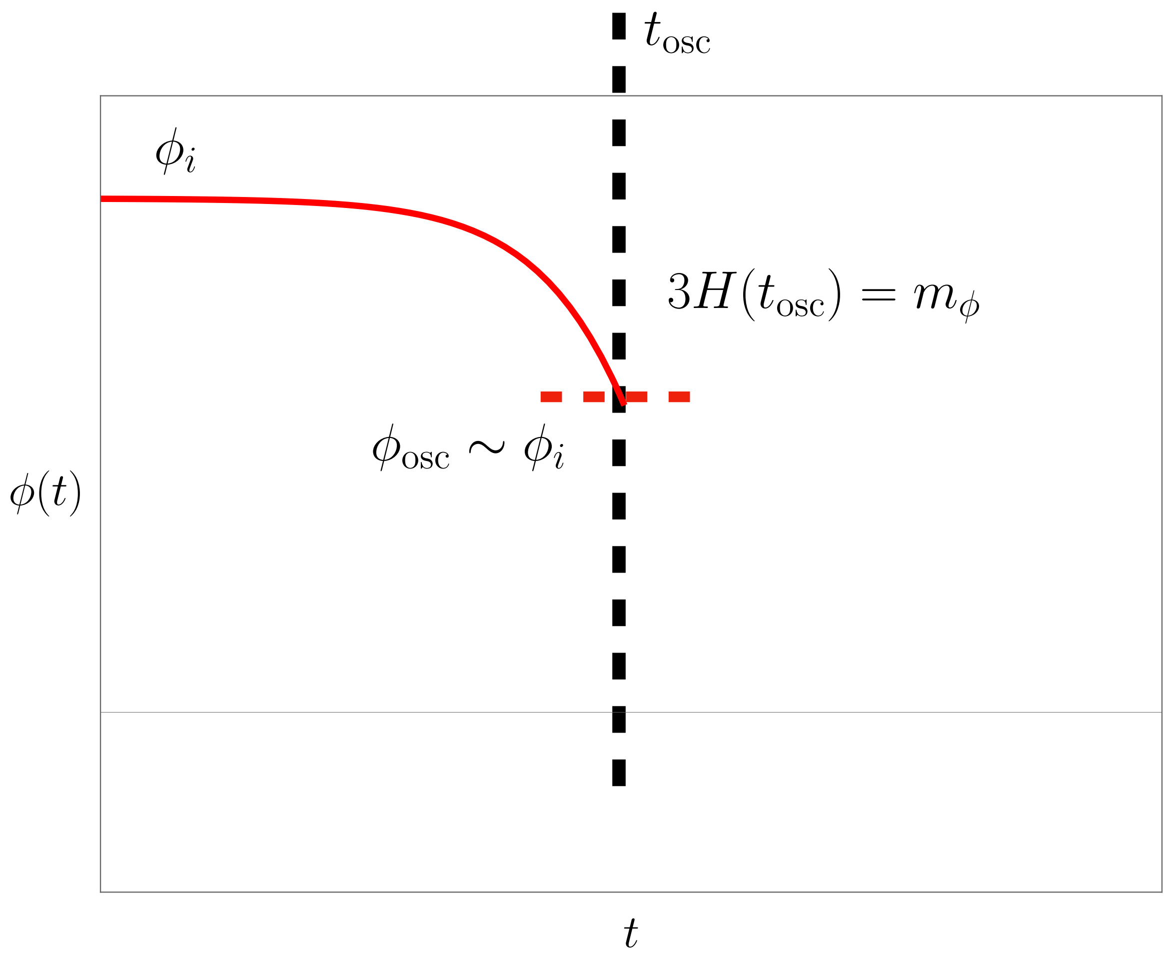

The classic misalignment mechanism

- At early times (high temperature) the scalar is held up by Hubble friction and remains approximately at its initial field value.
- As the universe cools, the Hubble eventually drops below the scalar mass. This signals the onset of scalar oscillations.
- At late times the scalar oscillates about its minimum and is also diluted due to Hubble expansion.

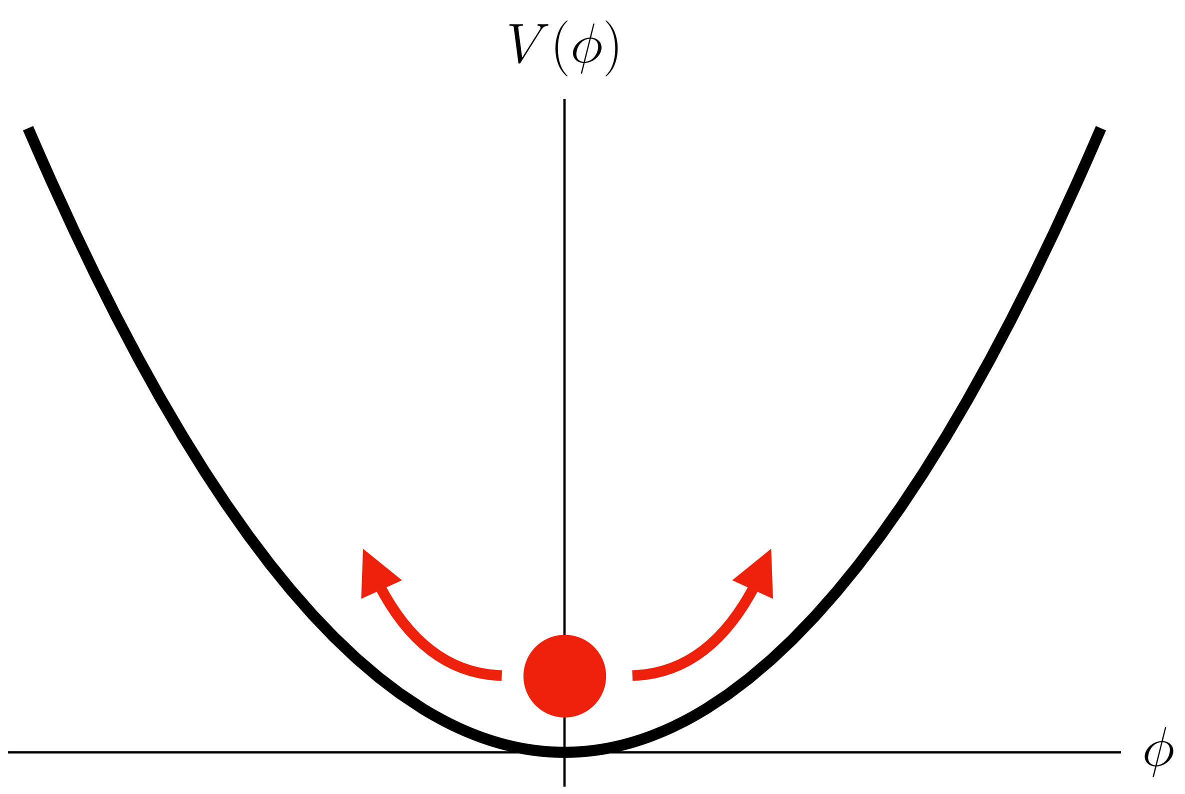

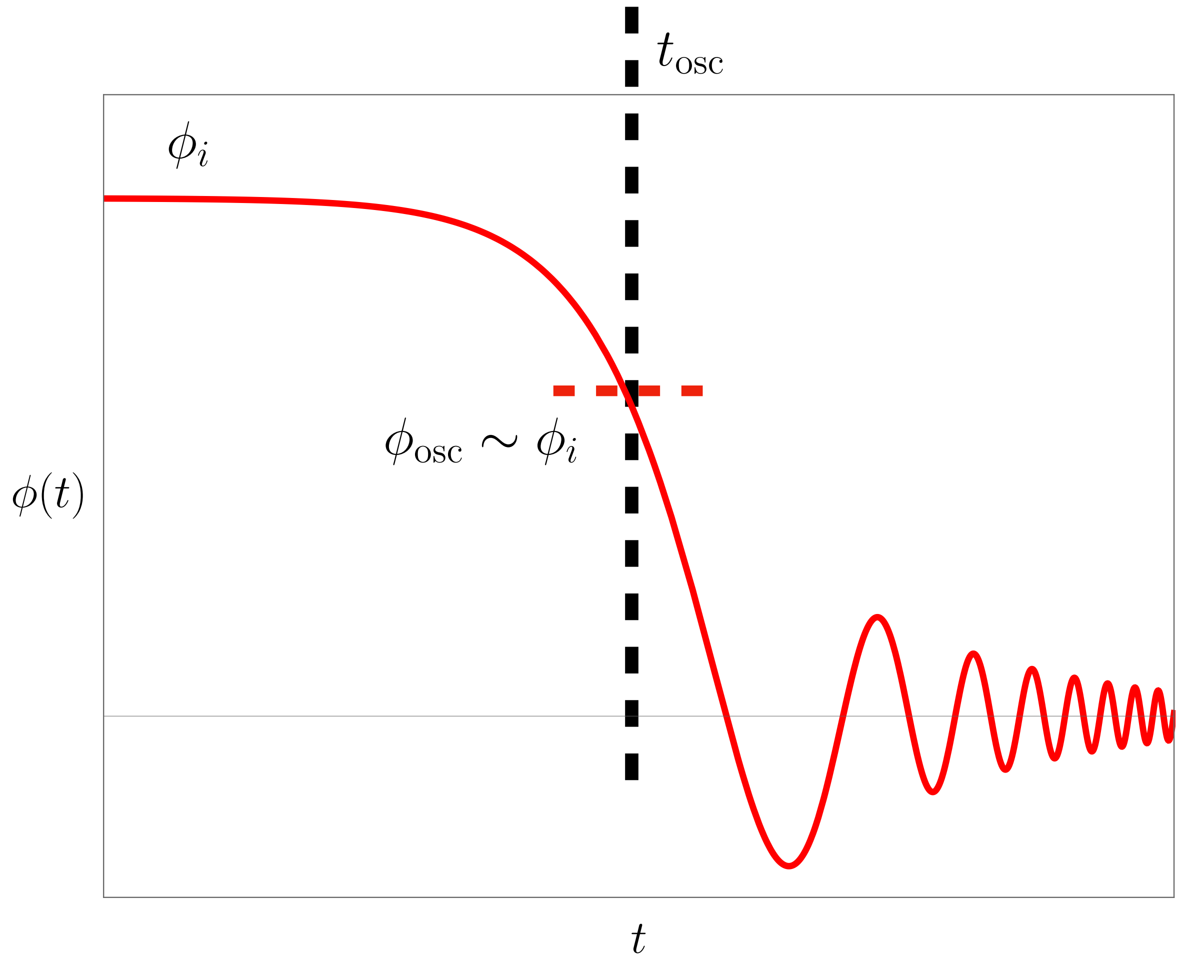

The classic misalignment mechanism

- At early times (high temperature) the scalar is held up by Hubble friction and remains approximately at its initial field value.
- As the universe cools, the Hubble eventually drops below the scalar mass. This signals the onset of scalar oscillations.
- At late times the scalar oscillates about its minimum and is also diluted due to Hubble expansion.

- The energy density stored in the scalar field redshifts like matter

$$\rho_\phi = \frac{1}{2} m_\phi \langle \phi^2(t) \rangle \sim a(t)^{-3} \sim t^{-3/2} \sim T^3$$

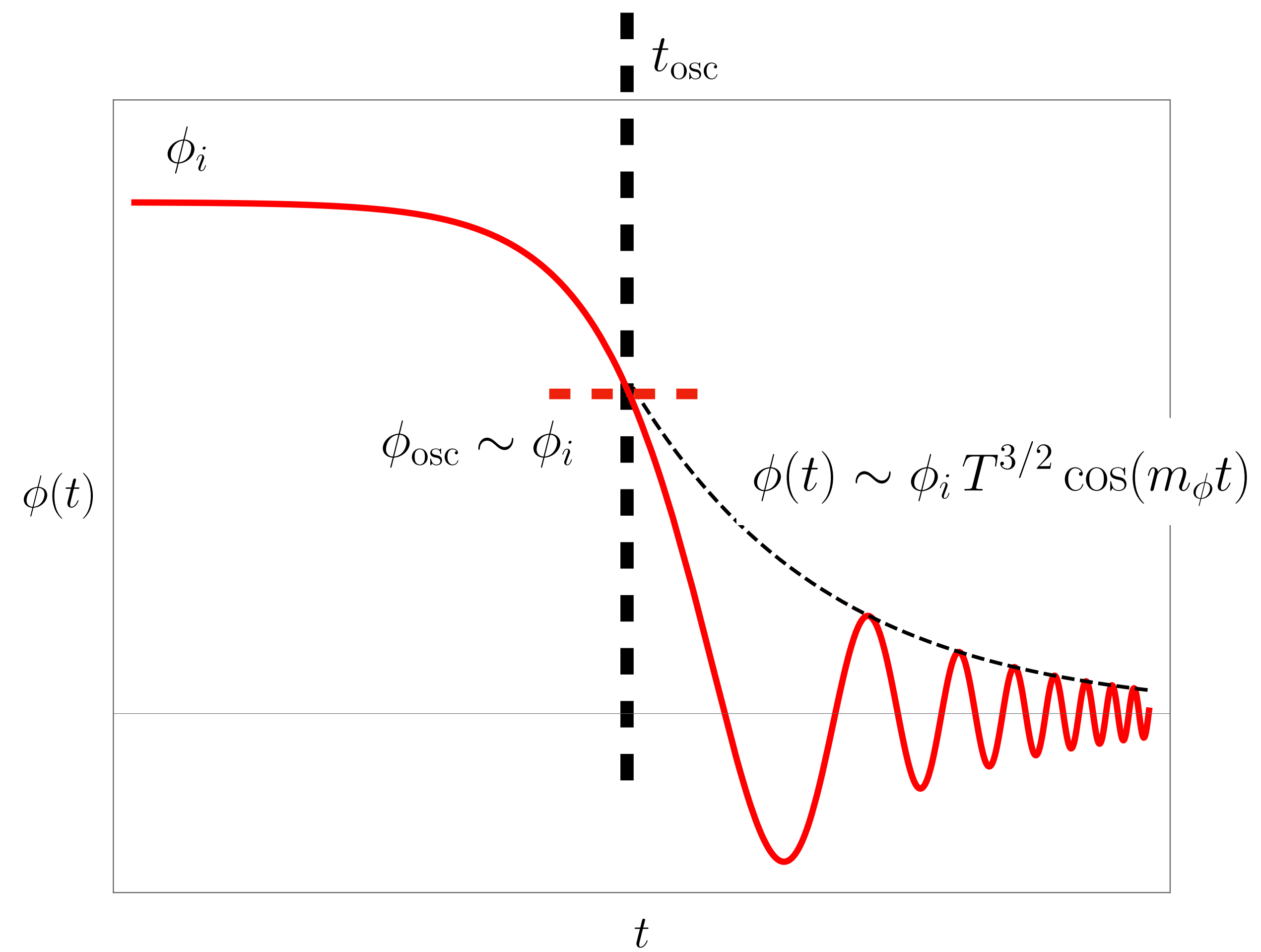

The classic misalignment mechanism

- At early times (high temperature) the scalar is held up by Hubble friction and remains approximately at its initial field value.
- As the universe cools, the Hubble eventually drops below the scalar mass. This signals the onset of scalar oscillations.
- At late times the scalar oscillates about its minimum and is also diluted due to Hubble expansion.

- The energy density stored in the scalar field redshifts like matter

$$\rho_\phi = \frac{1}{2} m_\phi \langle \phi^2(t) \rangle \sim a(t)^{-3} \sim t^{-3/2} \sim T^3$$

- The initial value of the field sets the amplitude of oscillations and controls the late time relic abundance

$$\Omega_\phi\Big|_0 = \frac{\rho_{\phi,0}}{\rho_{c,0}} \simeq \frac{\frac{1}{2} m_\phi^2 \phi_{\rm osc}^2 (T_0/T_{\rm osc})^3 (g_{*S}^0/g_{*S}^{\rm osc})}{\rho_{c,0}}$$

$$\approx 0.2 \left(\frac{m_\phi}{10^{-11}\,{\rm eV}}\right)^{1/2} \left(\frac{\phi_i/M_{\rm pl}}{10^{-4}}\right)^2$$

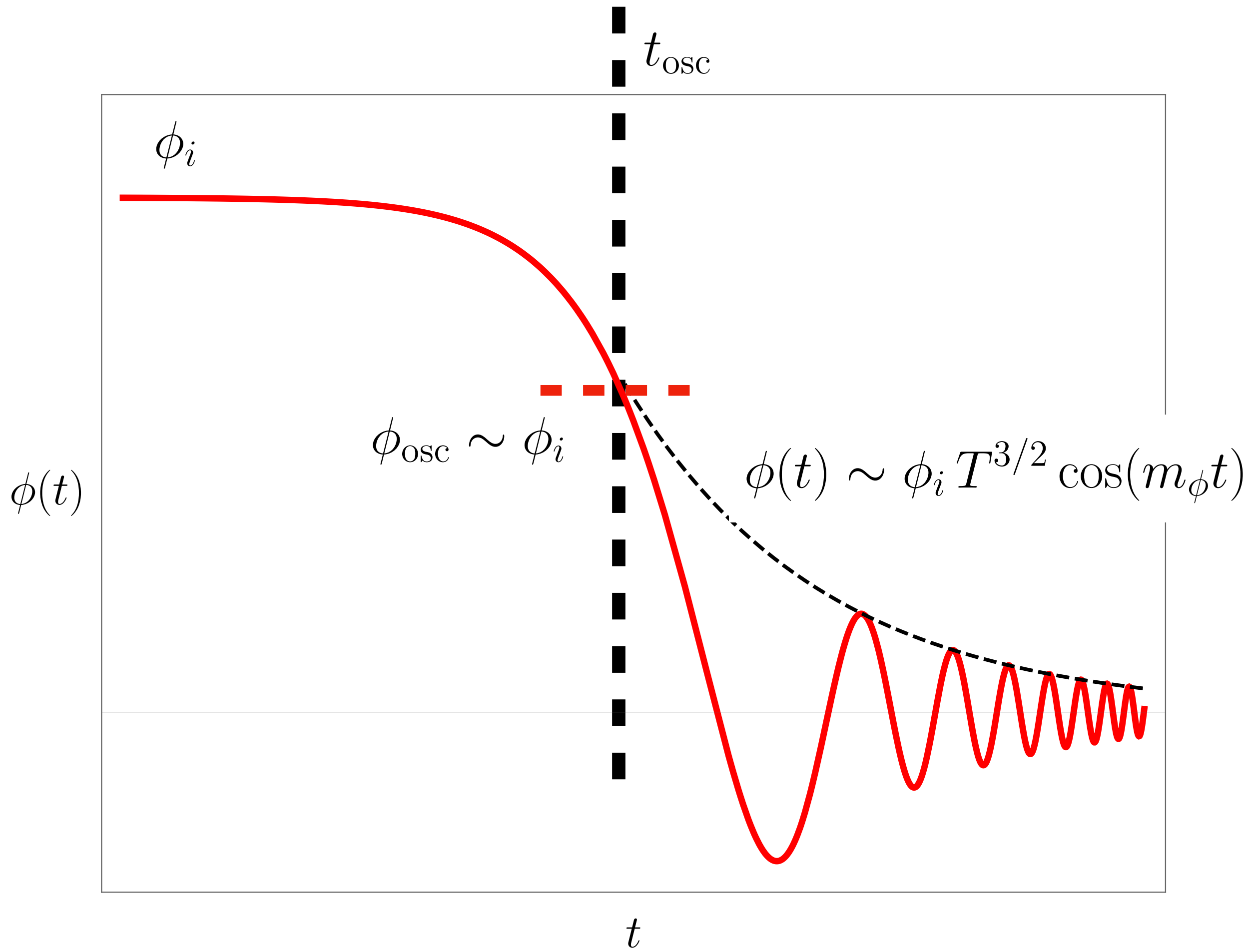

Thermal misalignment mechanism

[BB,Ghalsasi, 2109.04476]

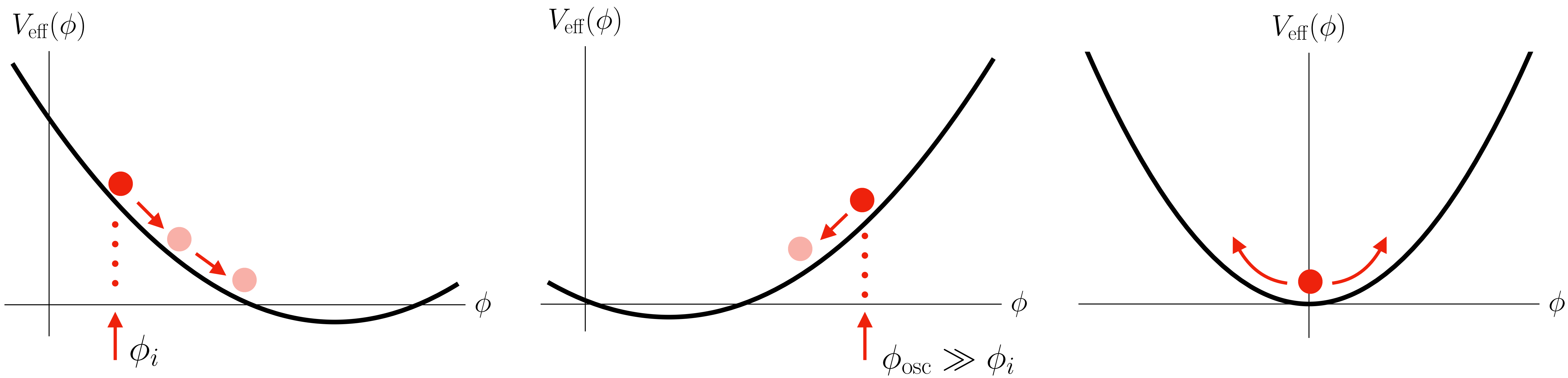

$T \gg m_\psi$ $T \sim T_{\rm osc}$ $T \ll m_\psi$

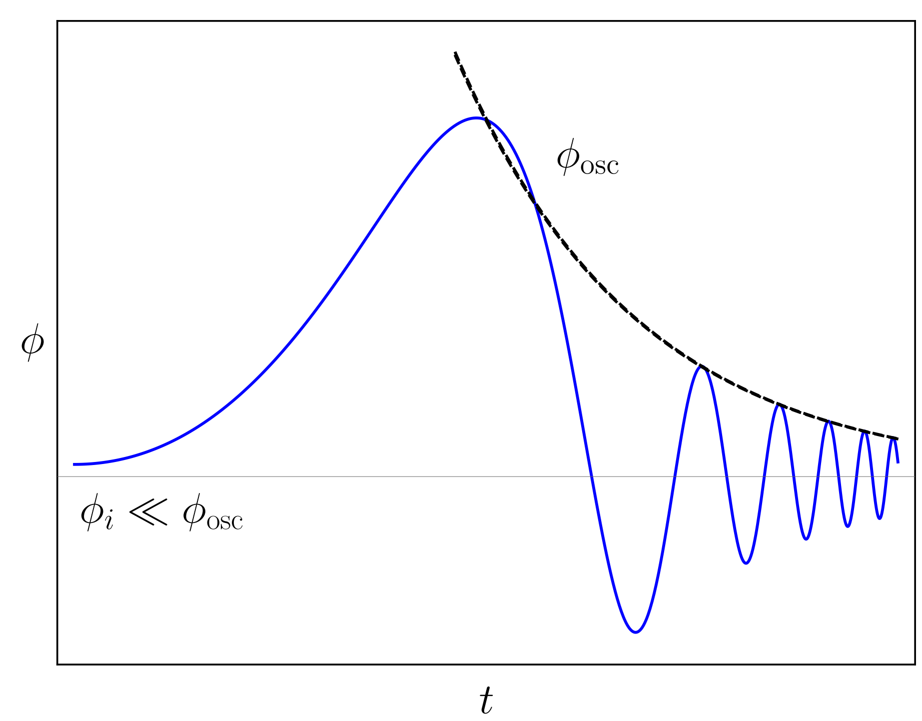

Thermal misalignment mechanism

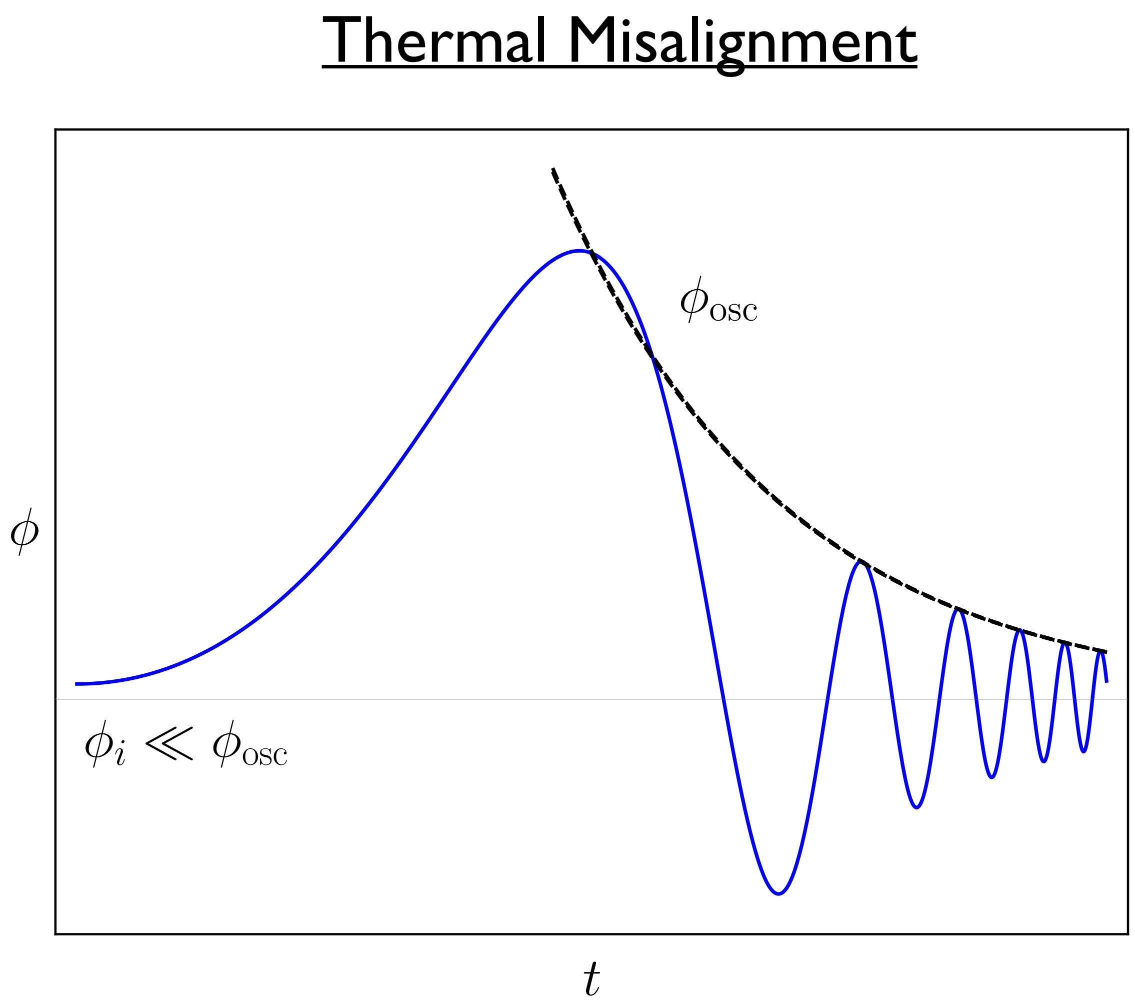

- At high temperatures, ϕ is dynamically misaligned from a small initial value to its oscillation amplitude

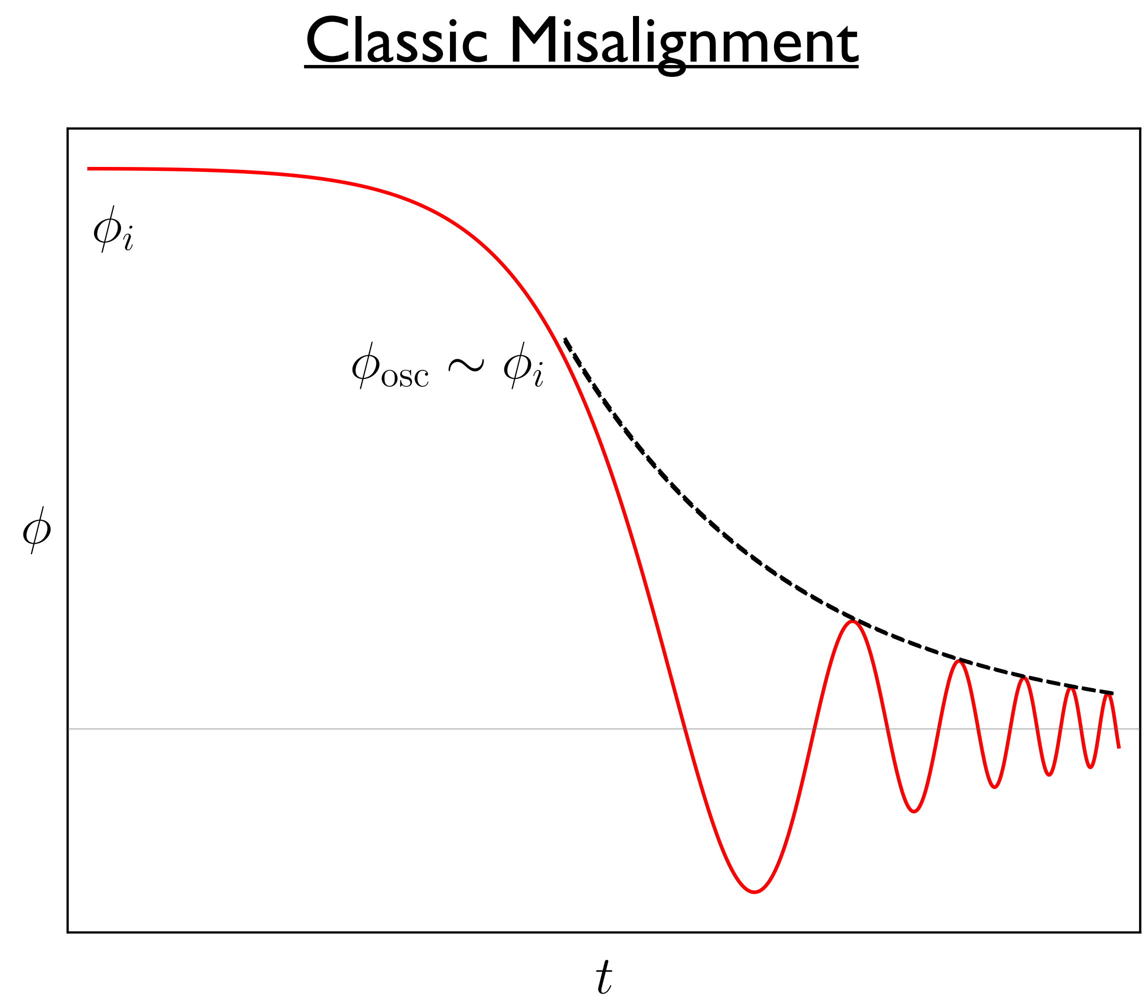

- ϕ oscillation amplitude and abundance dictated by initial conditions

Thermal misalignment mechanism

Thermal Misalignment

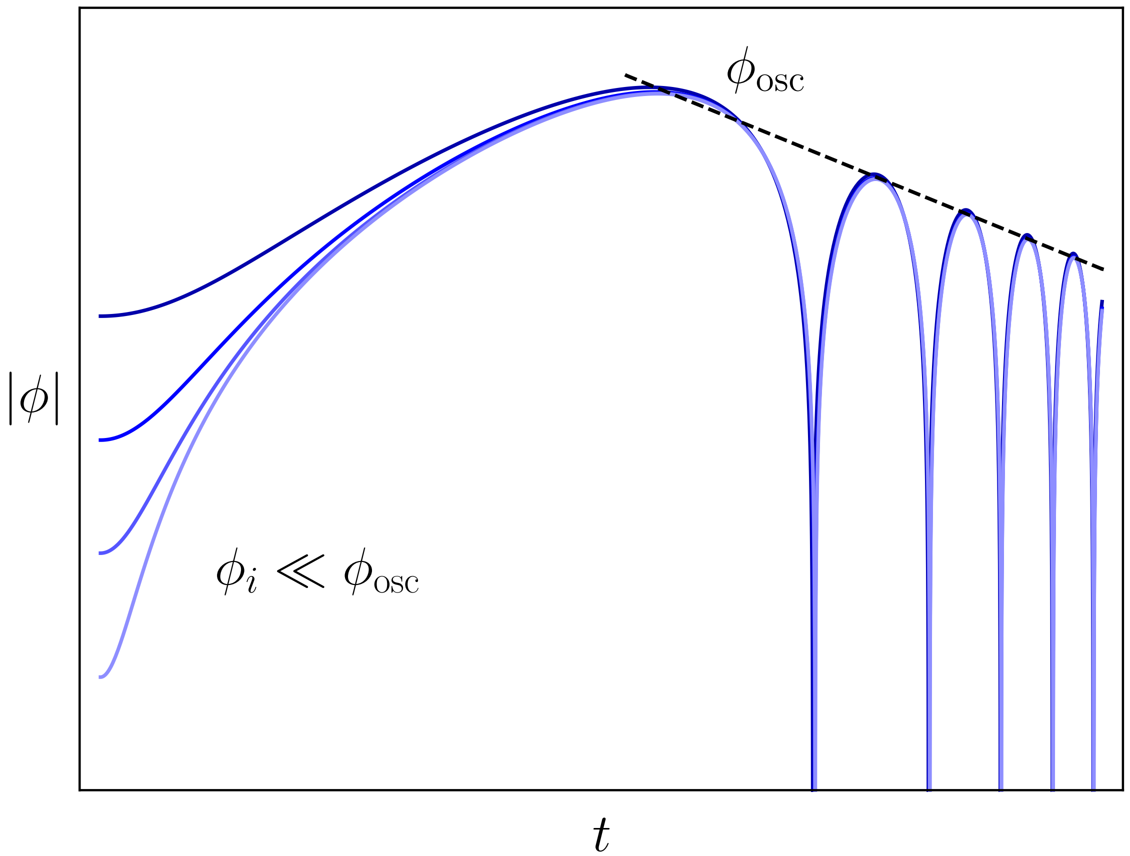

Classic Misalignment

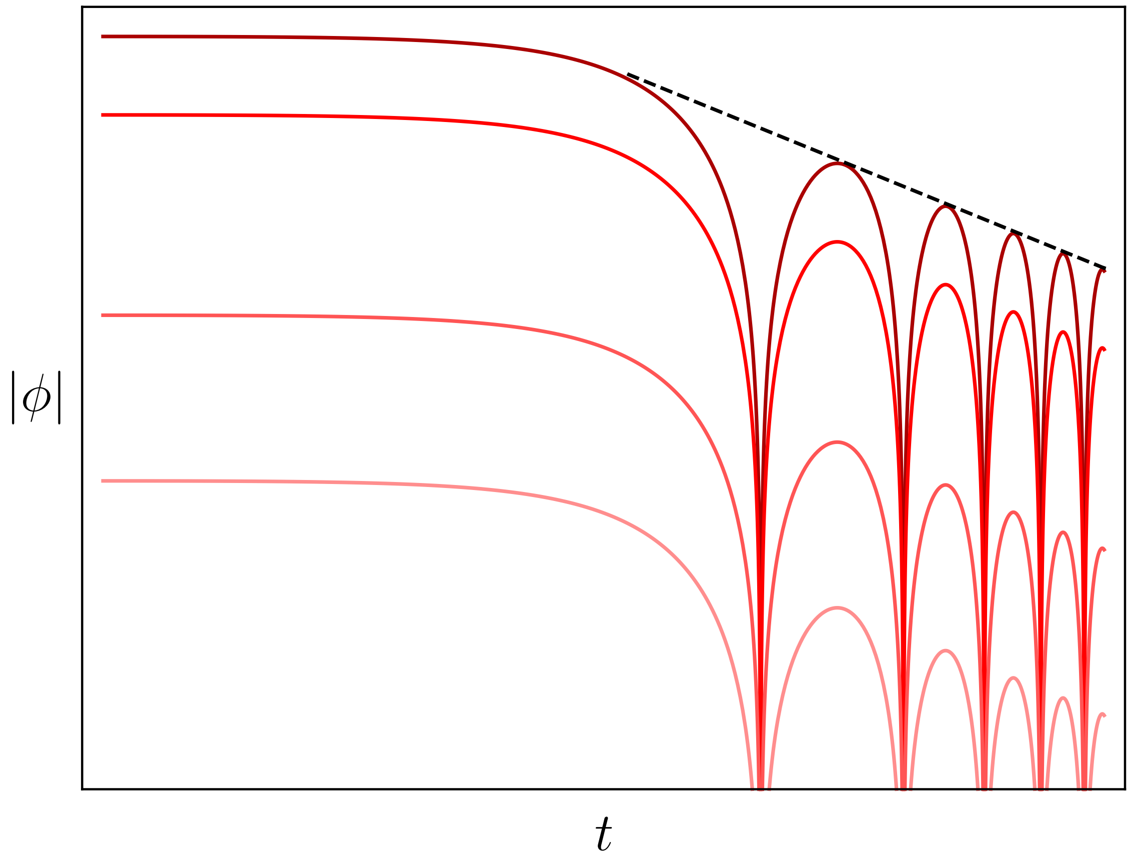

- At high temperatures, ϕ is dynamically misaligned from a small initial value to its oscillation amplitude
- The oscillation amplitude is an attractor for $\phi_i \ll \phi_{\rm osc}$ - insensitive to initial conditions

- ϕ oscillation amplitude and abundance dictated by initial conditions

Thermal misalignment mechanism

<u>Thermal Misalignment</u>

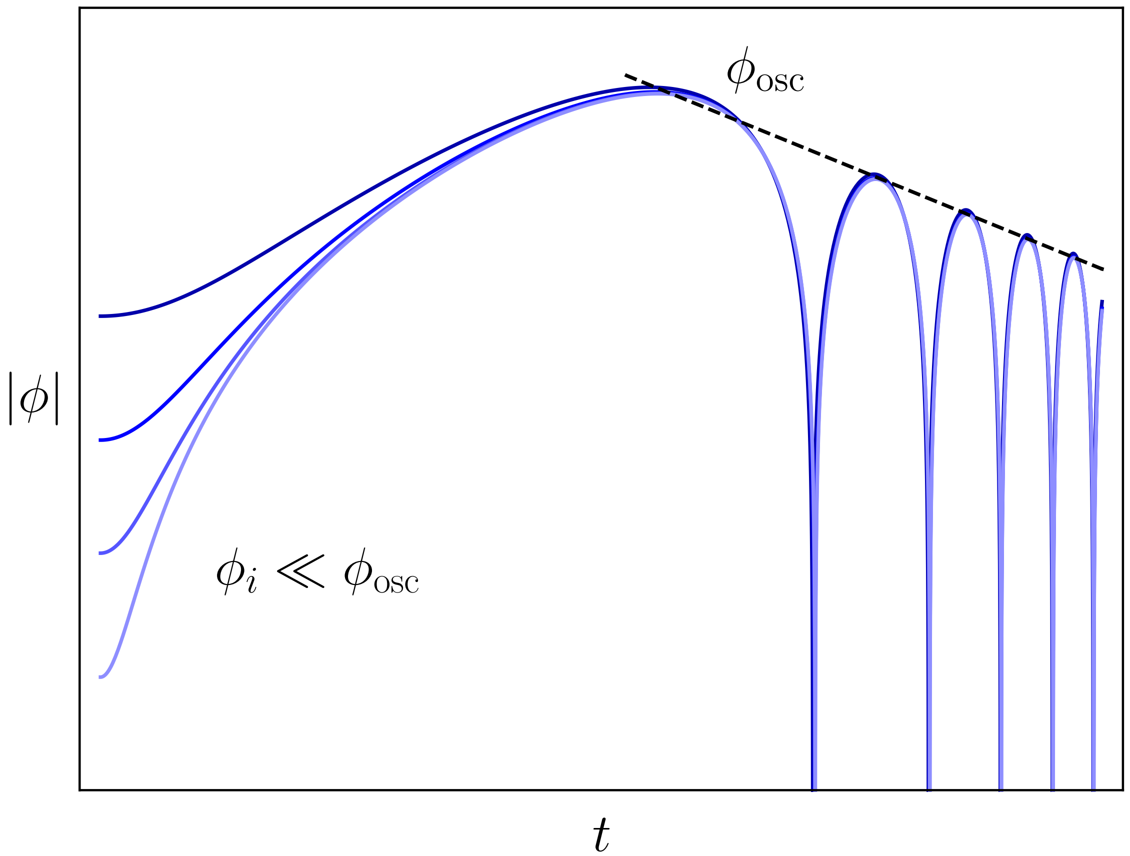

<u>Classic Misalignment</u>

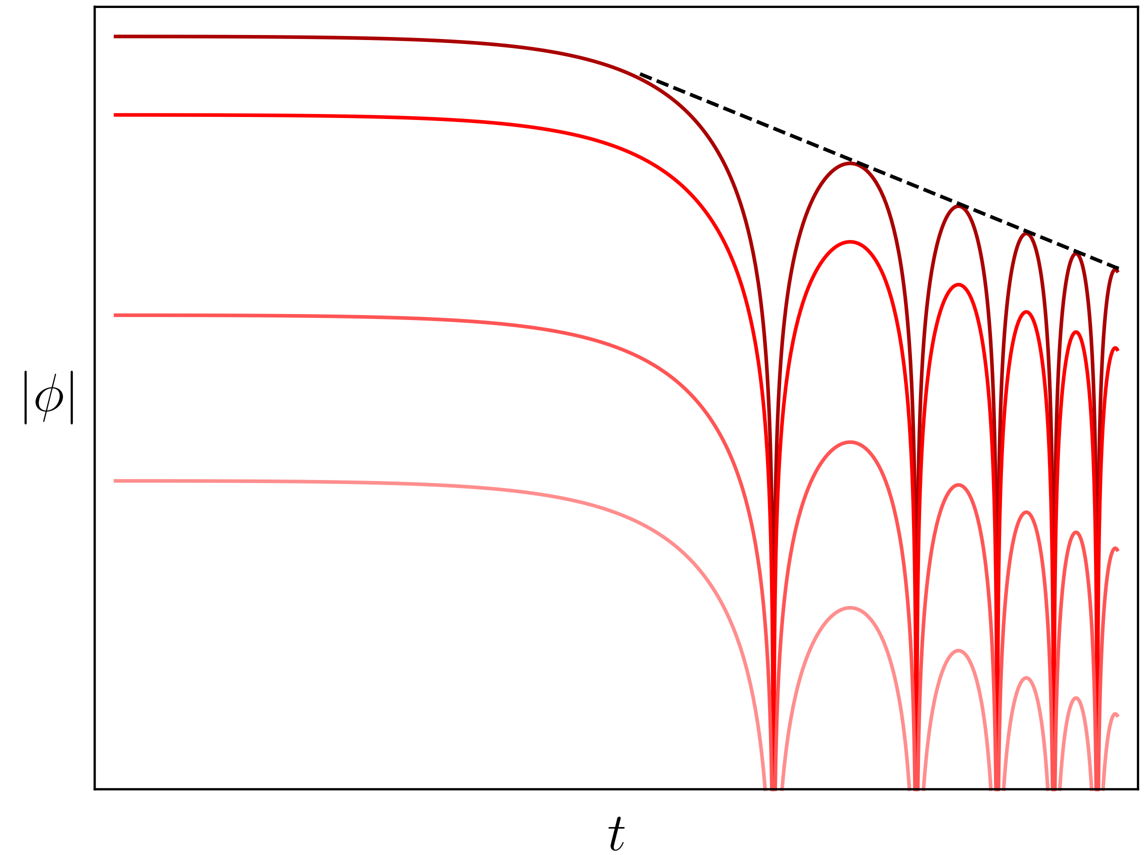

- At high temperatures, ϕ is dynamically misaligned from a small initial value to its oscillation amplitude
- The oscillation amplitude is an attractor for $\phi_i \ll \phi_{\rm osc}$ - insensitive to initial conditions
- The oscillation amplitude and resulting abundance is dictated by microscopic particle physics

- ϕ oscillation amplitude and abundance dictated by initial conditions

Basic model

- Consider a toy model with a scalar DM ϕ and a Dirac fermion ψ.
- The fermion is in thermal equilibrium with the plasma in the early universe
- The DM couples to the fermion through a Yukawa interaction. The Lagrangian is

$$
\begin{aligned}
-\mathcal{L} \supset & \frac{1}{2} m_\phi^2 \phi^2 + m_\psi \overline{\psi} \psi + \lambda \phi \overline{\psi} \psi \\
= & \frac{1}{2} m_\phi^2 \phi^2 + m_\psi \left(1 - \frac{\beta \phi}{M_{\rm pl}}\right) \overline{\psi} \psi
\end{aligned}
\qquad \lambda \equiv -\beta \frac{m_\psi}{M_{\rm pl}}
$$

- We will be interested in couplings β that are within a few orders of magnitude of unity. This means the Yukawa coupling is very feeble.
- Effective fermion mass in the scalar field background: $$m_\psi(\phi) = m_\psi + \lambda \phi = m_\psi \left(1 - \frac{\beta \phi}{M_{\rm pl}}\right)$$
- Fermion free energy density depends on scalar field background, giving rise to scalar effective potential

Effective potential

- To investigate the cosmological evolution of ϕ, we require the effective potential:

$$V_{\text{eff}}(\phi, T) = V_0(\phi) + V_1^0(\phi) + V_1^T(\phi)$$

- There are three contributions:
  - Tree level potential $$V_0(\phi) = \frac{1}{2}\, m_\phi^2 \phi^2$$
  - Coleman-Weinberg (zero temperature) $$V_1^0(\phi) = -g_\psi \frac{[m_\psi^2(\phi)]^2}{64\pi^2}\left[\log\left(\frac{m_\psi^2(\phi)}{\mu^2}\right) - \frac{3}{2}\right]$$ ($\overline{\text{MS}}$ scheme)
  - 1-loop finite temperature $$V_1^T(\phi) = -\frac{g_\psi}{2\pi^2} T^4 J_F\left[\frac{m_\psi^2(\phi)}{T^2}\right]$$

Integral: $$J_F(w^2) = \int_0^\infty dx\, x^2 \,\log[\,1 + e^{-\sqrt{x^2+w^2}}\,]$$

- For now, we neglect the influence of the Coleman-Weinberg potential
  - This implies a fine-tuning when the scalar is very light (usual hierarchy problem)
  - As we will see, much of the cosmologically motivated parameter space is not tuned

Evolution of potential with increasing temperature

$$V_{\text{eff}}(\phi, T) \simeq V_0(\phi) + V_1^T(\phi)$$

$$V_0(\phi) = \frac{1}{2} m_\phi^2 \phi^2$$

$$V_1^T(\phi) = -\frac{g_\psi}{2\pi^2} T^4 \int_0^\infty dx\, x^2 \log\left[1 + \exp\left(-\sqrt{x^2 + \frac{m_\psi(\phi)^2}{T^2}}\right)\right]$$

$$\sim e^{-m_\psi/T} \quad \text{for} \quad T \ll m_\psi$$

Boltzmann suppressed

Low temperature

$T = 0.1\, m_\psi$

- Tree level dominates at low temperature
- Finite temperature contribution suppressed

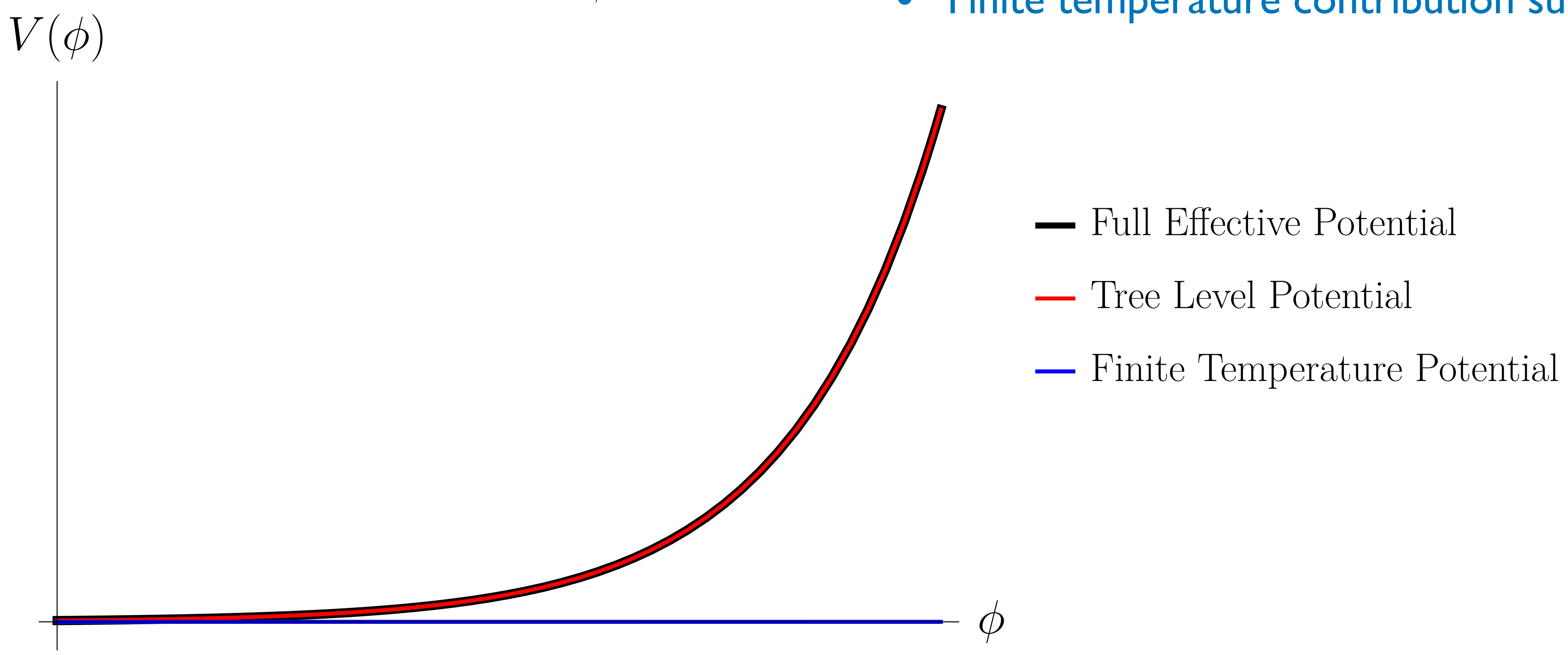

Evolution of potential with increasing temperature

$$V_{\rm eff}(\phi, T) \simeq V_0(\phi) + V_1^T(\phi) \quad \Longrightarrow \quad \begin{aligned} V_0(\phi) &= \frac{1}{2} m_\phi^2 \phi^2 \\ V_1^T(\phi) &= -\frac{g_\psi}{2\pi^2} T^4 \int_0^\infty dx\, x^2 \log\left[1 + \exp\left(-\sqrt{x^2 + \frac{m_\psi(\phi)^2}{T^2}}\right)\right] \end{aligned}$$

Intermediate temperature

$T = m_\psi$

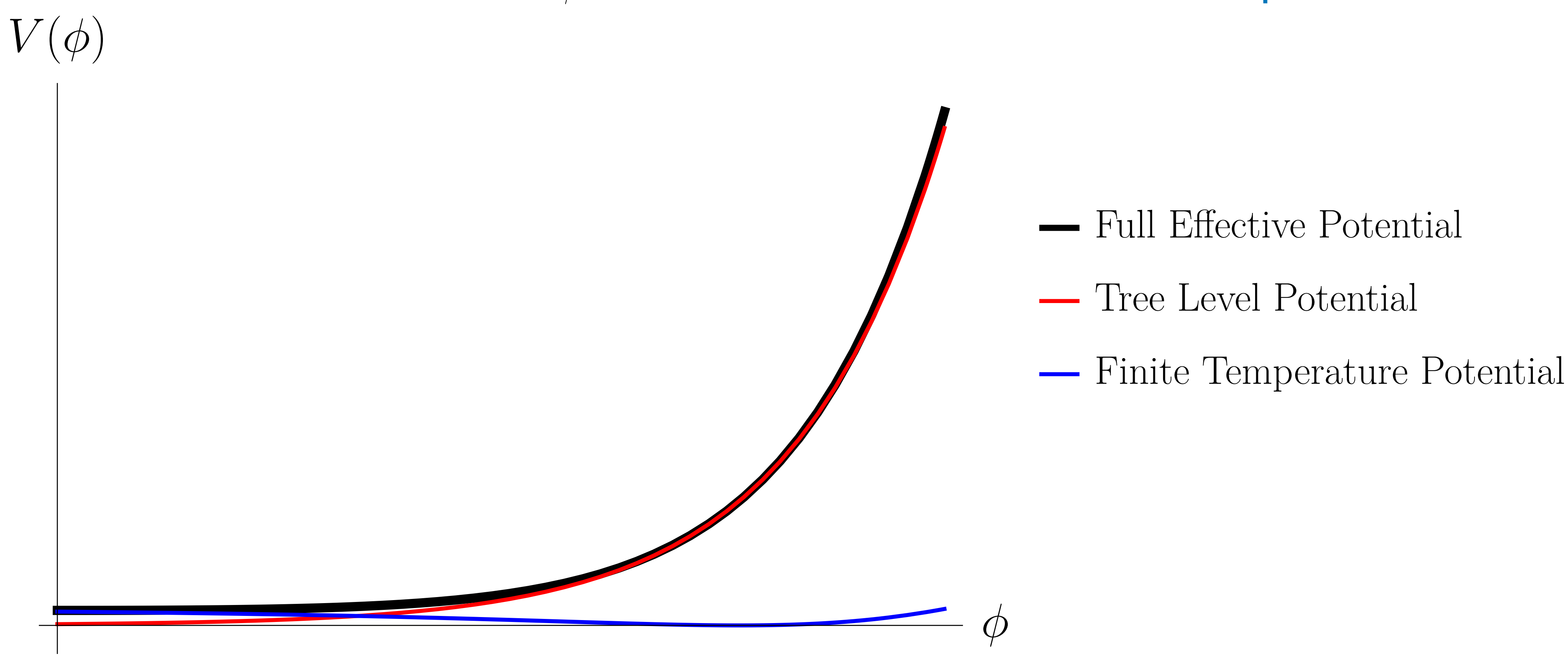

- Finite temperature contribution grows at intermediate temperatures

Evolution of potential with increasing temperature

$$V_{\text{eff}}(\phi, T) \simeq V_0(\phi) + V_1^T(\phi) \quad \Rightarrow$$

$$V_0(\phi) = \frac{1}{2} m_\phi^2 \phi^2$$

$$V_1^T(\phi) = -\frac{g_\psi}{2\pi^2} T^4 \int_0^\infty dx\, x^2 \log\left[1 + \exp\left(-\sqrt{x^2 + \frac{m_\psi(\phi)^2}{T^2}}\right)\right]$$

$$\sim \frac{T^2 m_\psi^2}{12}\left(1 - \frac{\beta\,\phi}{M_{\text{pl}}}\right)^2 \quad \text{for} \quad T \gg m_\psi$$

Minimum at $\phi \sim M_{\text{pl}}/\beta$

<u>High temperature</u>

$T = 3\, m_\psi$

- Finite temperature piece dominates at high temperatures
- Potential minimum located at large scalar field values

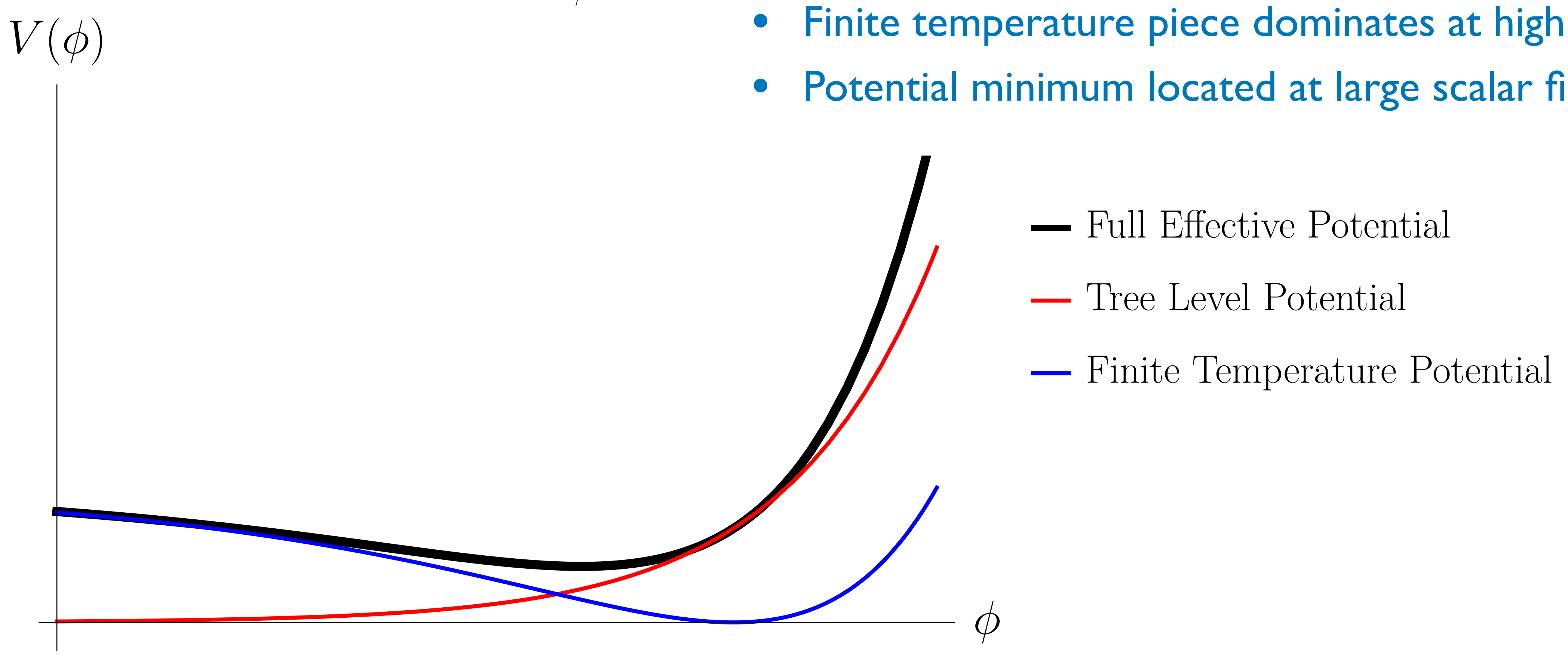

Evolution of potential with increasing temperature

$$V_{\rm eff}(\phi, T) \simeq V_0(\phi) + V_1^T(\phi) \quad \rightarrow \quad V_0(\phi) = \frac{1}{2} m_\phi^2 \phi^2$$

$$V_1^T(\phi) = -\frac{g_\psi}{2\pi^2} T^4 \int_0^\infty dx\, x^2 \log\left[1 + \exp\left(-\sqrt{x^2 + \frac{m_\psi(\phi)^2}{T^2}}\right)\right]$$

$$\sim \frac{T^2 m_\psi^2}{12}\left(1 - \frac{\beta\,\phi}{M_{\rm pl}}\right)^2 \quad \text{for} \quad T \gg m_\psi$$

↳ Minimum at $\phi \sim M_{\rm pl}/\beta$

<u>High temperature</u>

$T = 10\, m_\psi$

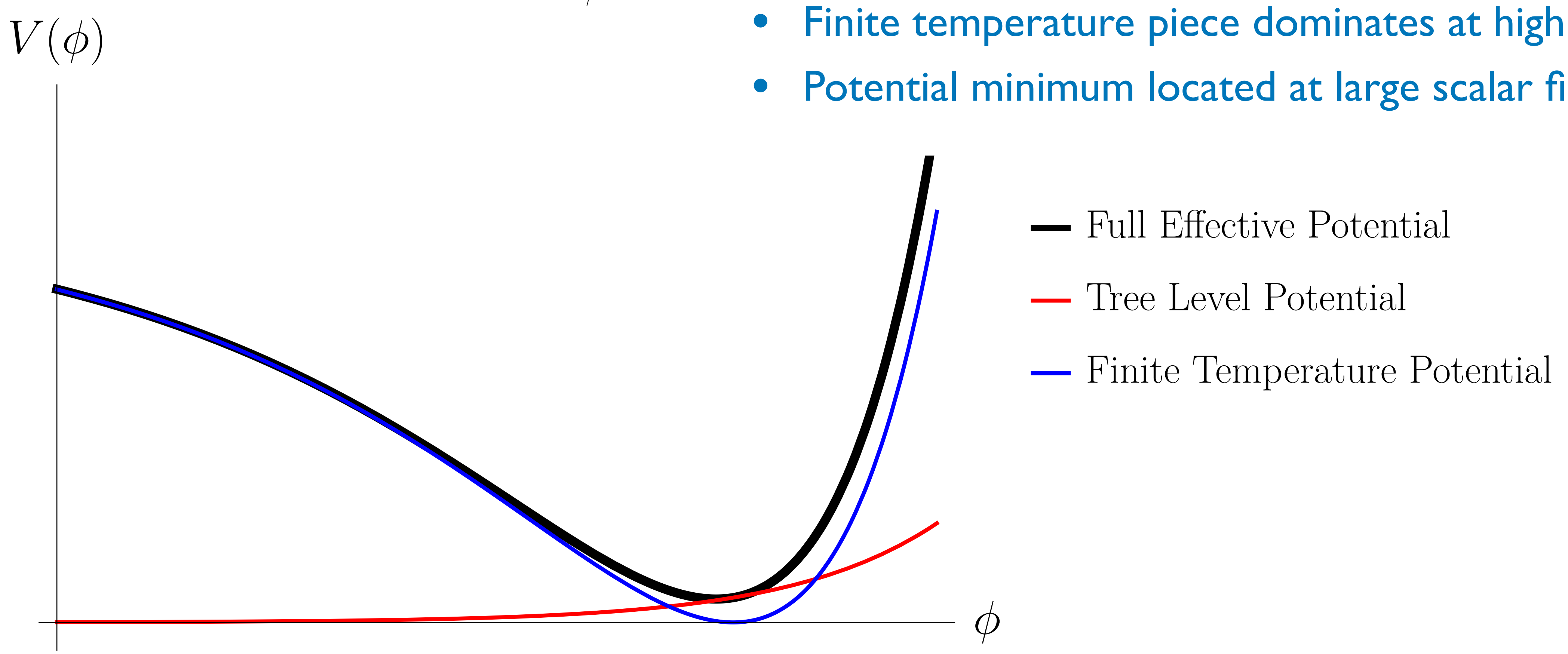

- Finite temperature piece dominates at high temperatures
- Potential minimum located at large scalar field values

Cartoon sketch of the mechanism

- Assume nonzero homogeneous scalar field with arbitrary* initial condition after inflation
- In the case of a Standard Model fermion, initial condition set after electroweak phase transition

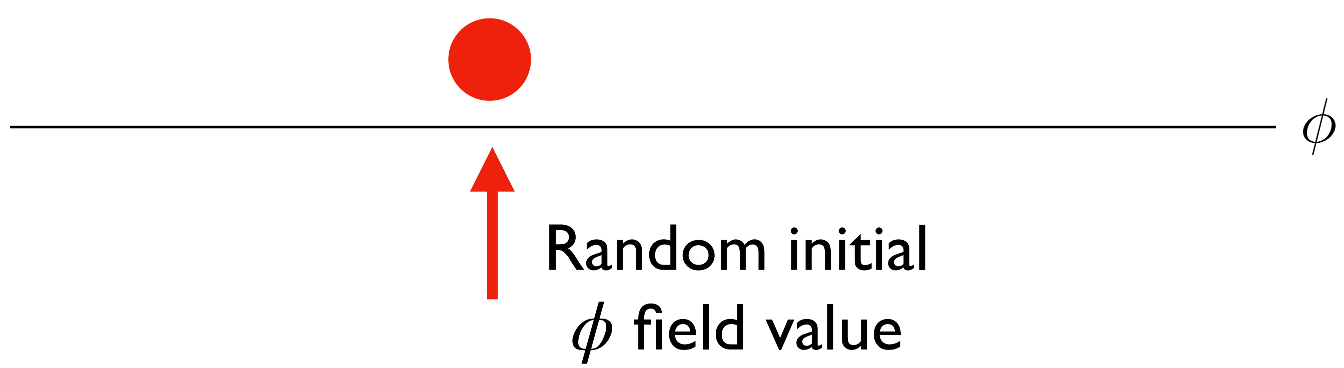

* Caveats will be discussed below

Cartoon sketch of the mechanism

- Inflation ends and reheating occurs, creating the thermal plasma.
- The finite temperature potential dominates at this stage.
- ϕ rolls toward the minimum at large field values, generating misalignment

High temperature

$T \gg m_f$

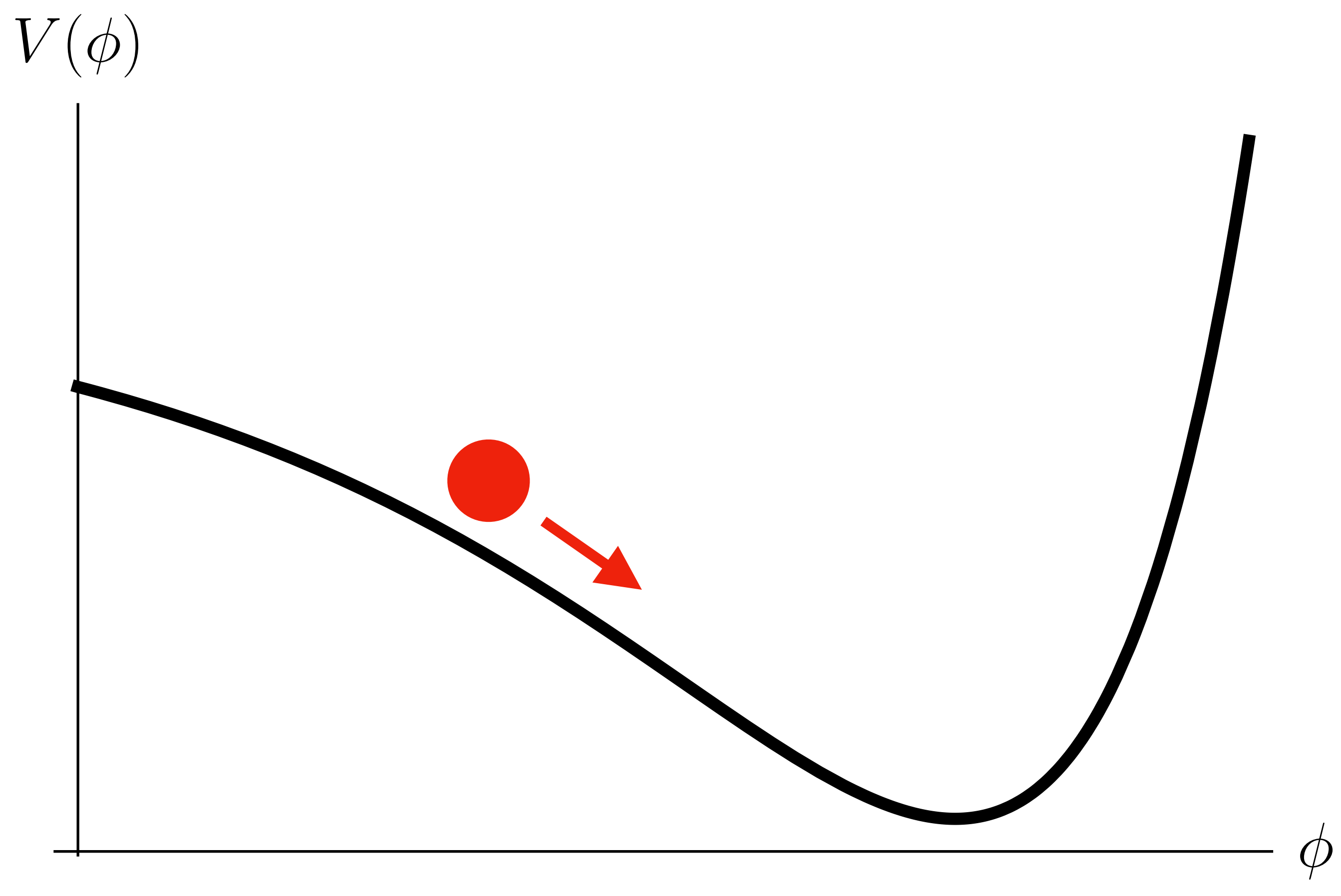

Cartoon sketch of the mechanism

- Inflation ends and reheating occurs, creating the thermal plasma.
- The finite temperature potential dominates at this stage.
- ϕ rolls toward the minimum at large field values, generating misalignment

<u>High temperature</u>

$T \gg m_f$

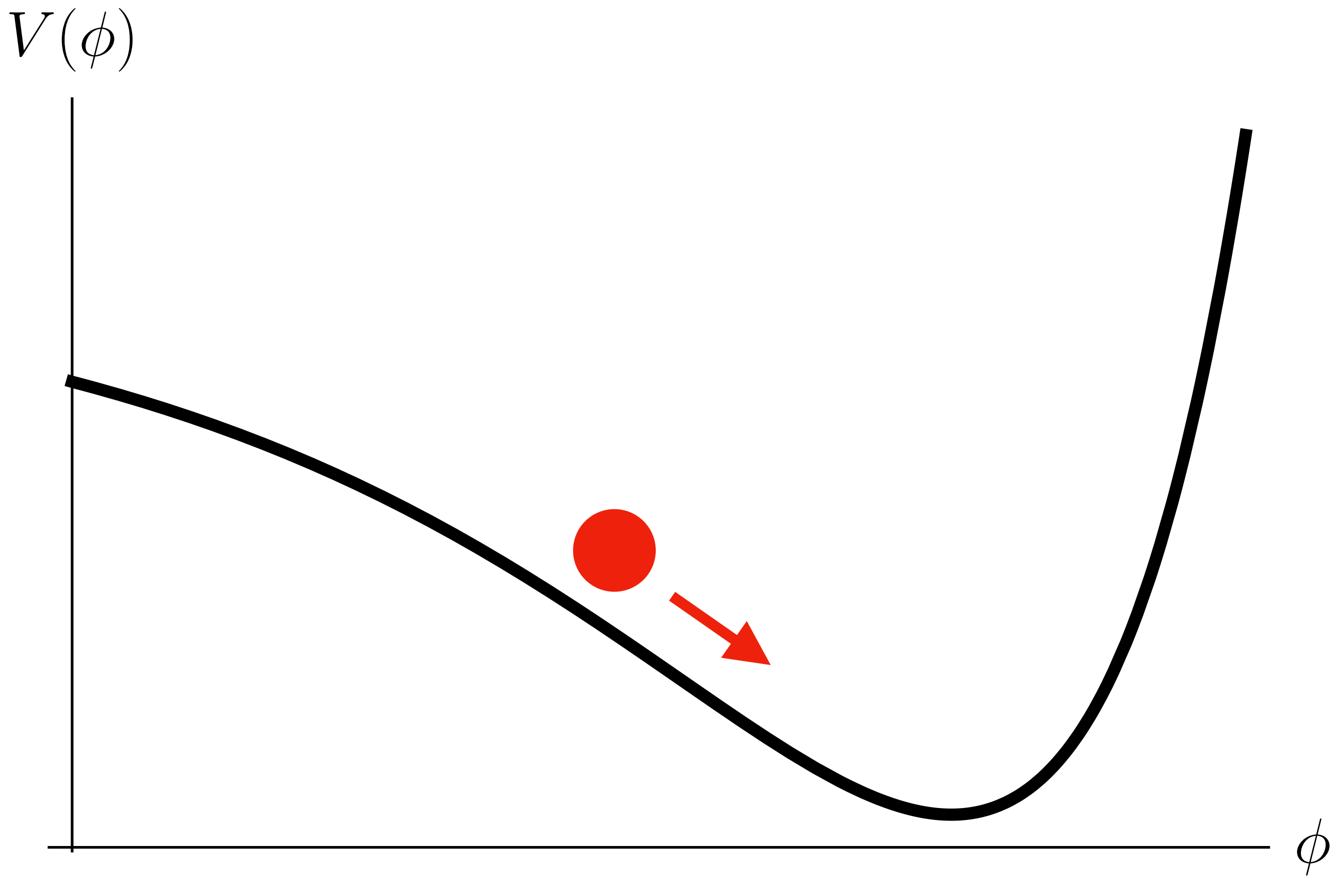

Cartoon sketch of the mechanism

- Inflation ends and reheating occurs, creating the thermal plasma.
- The finite temperature potential dominates at this stage.
- ϕ rolls toward the minimum at large field values, generating misalignment

High temperature

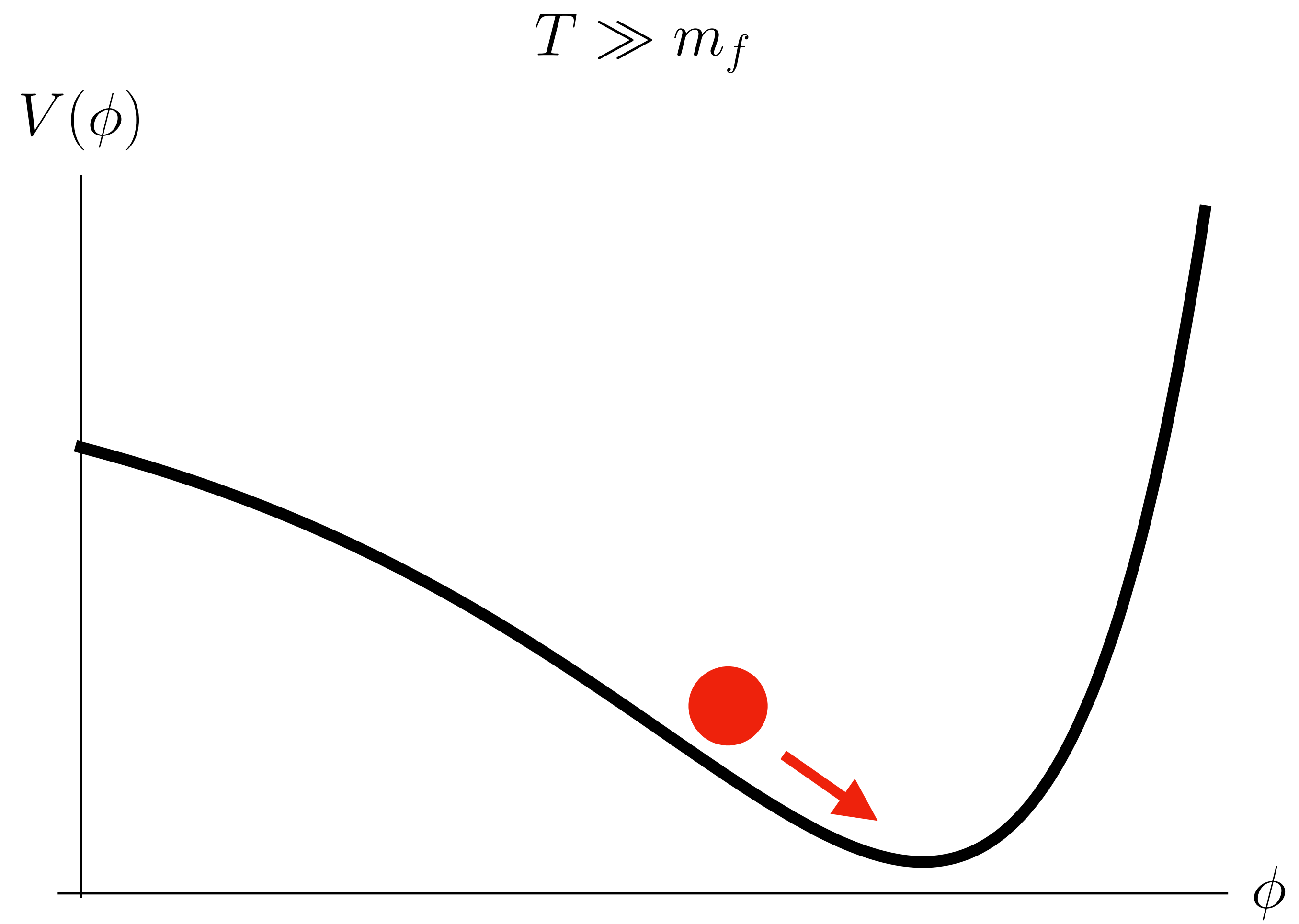

Cartoon sketch of the mechanism

- At intermediate temperatures of order the fermion mass, the finite temperature pieces becomes smaller.
- The minimum moves toward the origin

<u>Intermediate temperature</u>

$T \sim m_f$

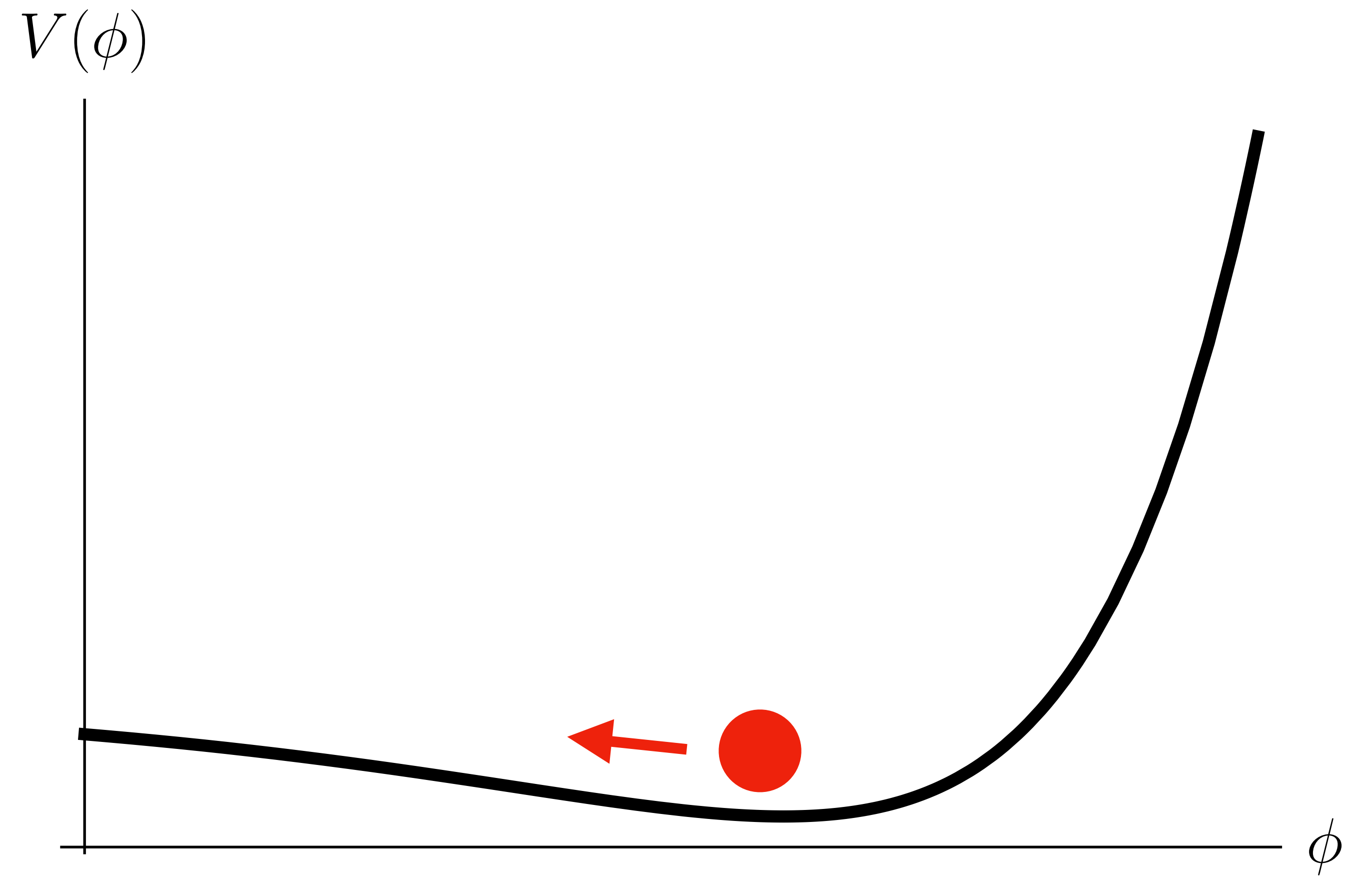

Cartoon sketch of the mechanism

- At intermediate temperatures of order the fermion mass, the finite temperature pieces becomes smaller.
- The minimum moves toward the origin

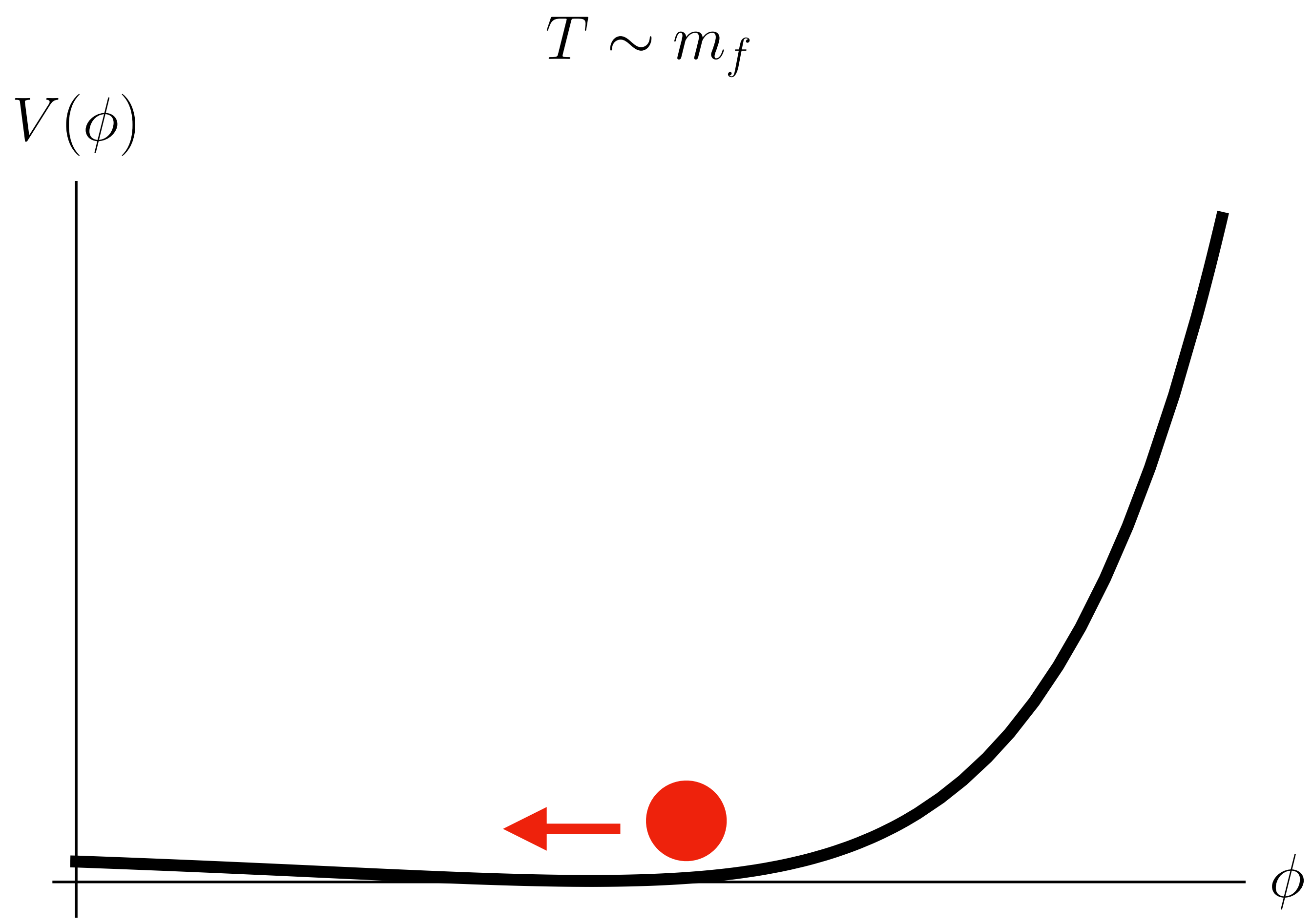

Cartoon sketch of the mechanism

- At low temperatures the tree level potential dominates
- The minimum is located at the origin
- Eventually ϕ oscillates and behaves as dark matter

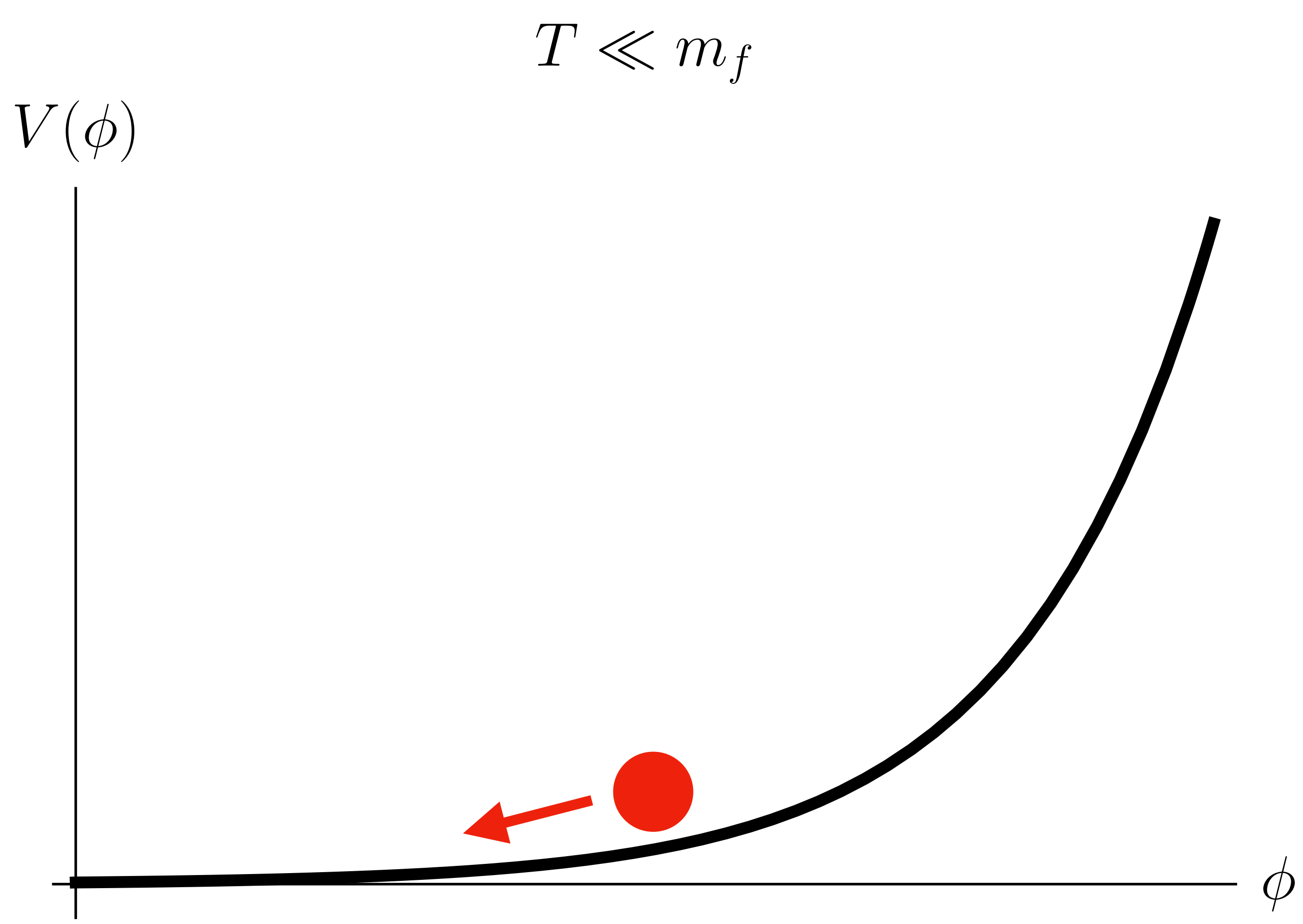

Cartoon sketch of the mechanism

- At low temperatures the tree level potential dominates
- The minimum is located at the origin
- Eventually ϕ oscillates and behaves as dark matter

$T \ll m_f$

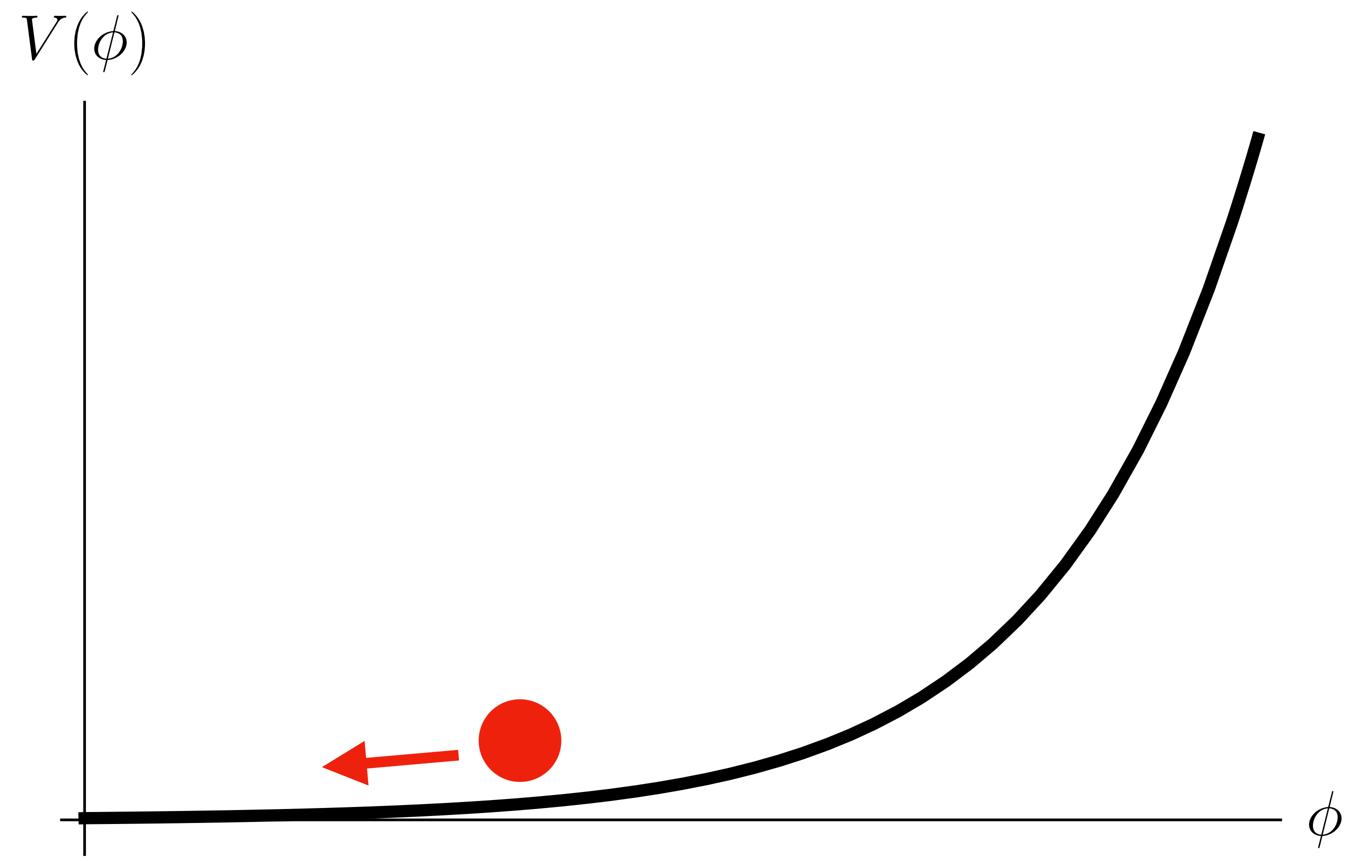

Cartoon sketch of the mechanism

- At low temperatures the tree level potential dominates
- The minimum is located at the origin
- Eventually ϕ oscillates and behaves as dark matter

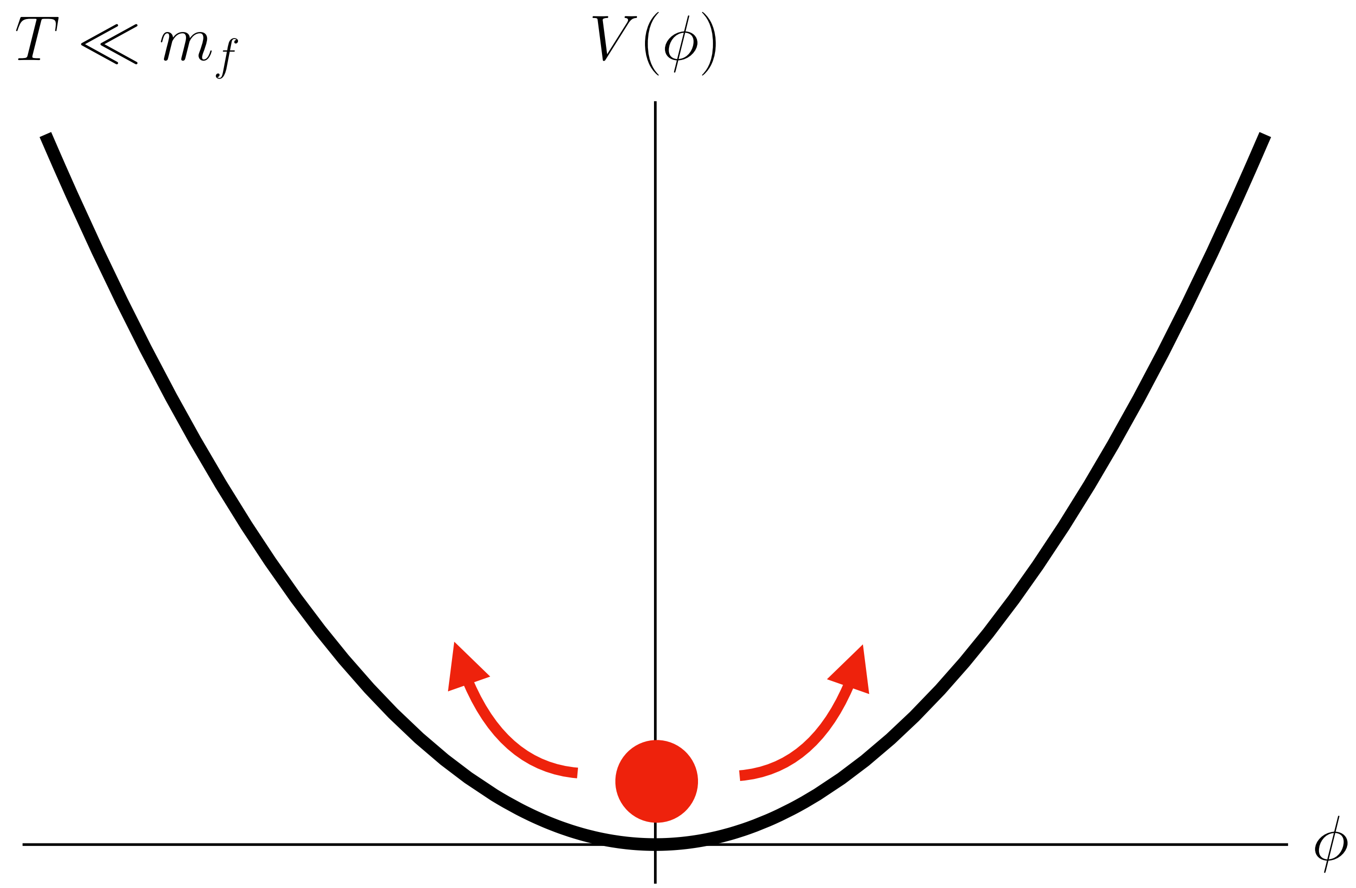

Evolution of scalar dark matter

- Equation of motion for ϕ : $$\ddot{\phi} + 3H\dot{\phi} + \frac{dV_{\mathrm{eff}}}{d\phi} = 0$$

- V_{eff} depends on $\dfrac{m_\psi(\phi)}{T} = \dfrac{m_\psi}{T}\left(1 - \dfrac{\beta\phi}{M_{\mathrm{pl}}}\right)$

➡ Change dependent variable to $y \equiv \dfrac{T}{m_\psi}$ (proxy for time or temperature)

- Introduce dimensionless parameter $\kappa \equiv \dfrac{m_\phi M_{\mathrm{pl}}}{m_\psi^2}$ (proxy for the DM mass)

- Equation of motion: $$\frac{d^2\phi}{dy^2} + \frac{\kappa^2}{\gamma^2 y^6}\left[\phi - \frac{g_\psi}{2\pi^2}\frac{y^2 M_{\mathrm{pl}}}{\kappa^2}\beta\left(1 - \frac{\beta\,\phi}{M_{\mathrm{pl}}}\right)\int_0^\infty dx\,\frac{x^2}{(1+e^\xi)\xi}\right] = 0$$

$$\xi = \sqrt{x^2 + \frac{1}{y^2}\left(1 - \frac{\beta\,\phi}{M_{\mathrm{pl}}}\right)^2}$$

➡ Equation of motion depends only on model parameters β and κ

- Given the model parameters and initial conditions, we can solve the equation of motion to determine $\phi(y)$

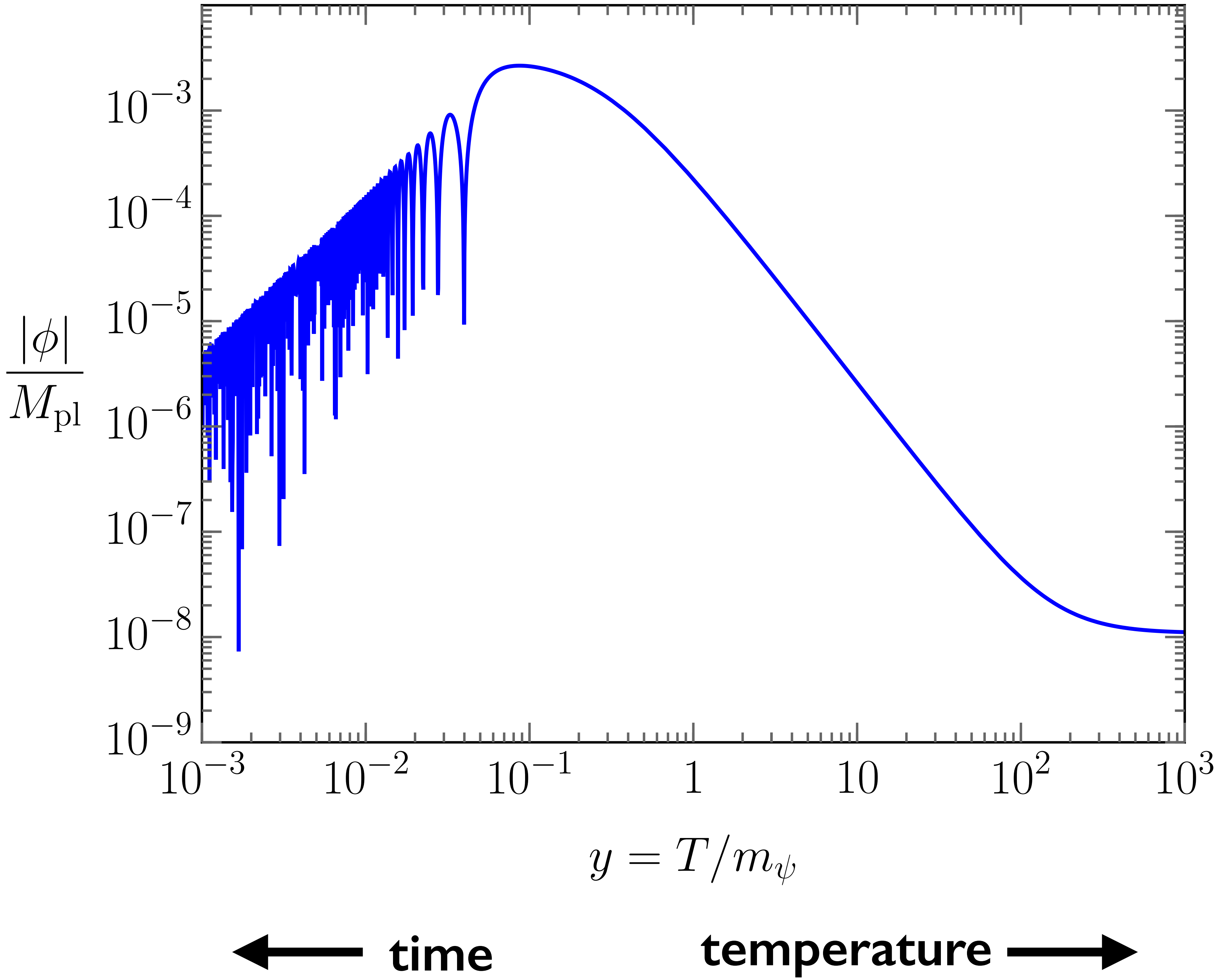
10^{-3}
10^{-4}
10^{-5}
10^{-6}
10^{-7}
10^{-8}
10^{-9}
$\frac{|\phi|}{M_{\rm pl}}$
10^{-3}
10^{-2}
10^{-1}
1
10
10^{2}
10^{3}
$y = T/m_\psi$
time
temperature

Effective potential analysis

- Effective potential at high temperatures:

$$V_{\text{eff}} \simeq \frac{1}{2} m_\phi^2 \phi^2 + \frac{T^2 m_\psi^2}{12}\left(1 - \frac{\beta\,\phi}{M_{\text{pl}}}\right)^2 = m_\psi^4 \left\{ \frac{1}{2}\kappa^2 \left(\frac{\phi}{M_{\text{pl}}}\right)^2 + \frac{y^2}{12}\left[1 - \beta\left(\frac{\phi}{M_{\text{pl}}}\right)\right]^2 \right\}$$

- Minimize potential

$$\phi_{\min} \simeq M_{\text{pl}} \left[\frac{\beta\, y^2}{\beta^2 y^2 + 6\,\kappa^2}\right] \simeq \begin{cases} \dfrac{M_{\text{pl}}}{\beta} & \text{for} \quad y \gg \dfrac{\sqrt{6}\,\kappa}{\beta} & \text{High } T \\ M_{\text{pl}} \dfrac{\beta\, y^2}{6\,\kappa^2} & \text{for} \quad y \ll \dfrac{\sqrt{6}\,\kappa}{\beta} & \text{Lower } T\text{, but } y_{\text{eff}} > 1 \end{cases}$$

$T \gg m_f$

- The scalar will initially evolve towards the minimum at large field values

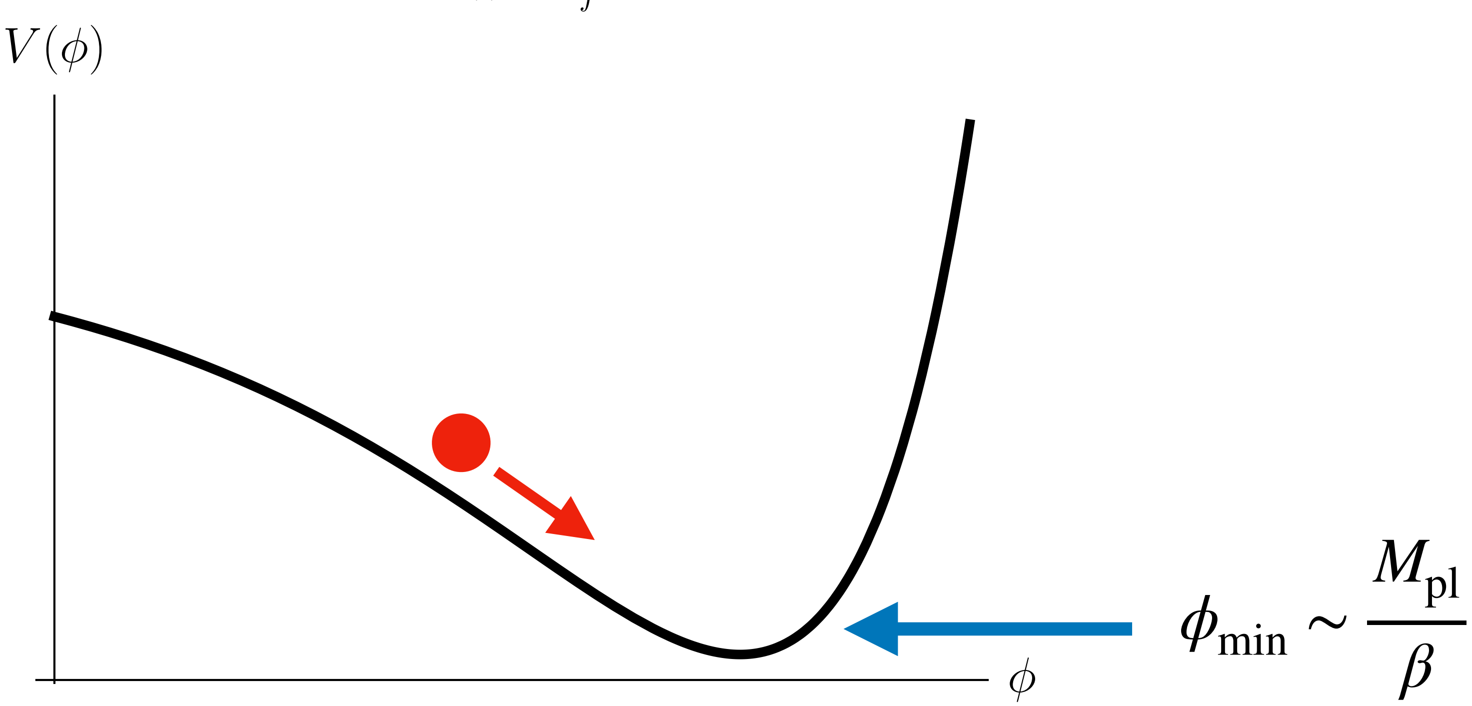

Initial trajectory

- Initial evolution caused by linear term in the effective potential

$$V_{\text{eff}} \supset -\frac{T^2 m_\psi^2}{6}\frac{\beta\,\phi}{M_{\text{pl}}}$$

- The scalar field "slow rolls" toward its minimum at large field values

$$|\ddot{\phi}| \ll |H\dot{\phi}| \quad \Rightarrow \quad \dot{\phi} = \frac{\beta m_\psi^2}{18\gamma} = \text{const.}$$

- The solution is given by

$$\phi(t) = \phi_i + \frac{\beta m_\psi^2}{18\gamma}(t - t_i)$$
$$\simeq \frac{\beta m_\psi^2}{18\gamma} t = \frac{\beta M_{\text{pl}}}{36\gamma^2}\frac{1}{y^2}$$

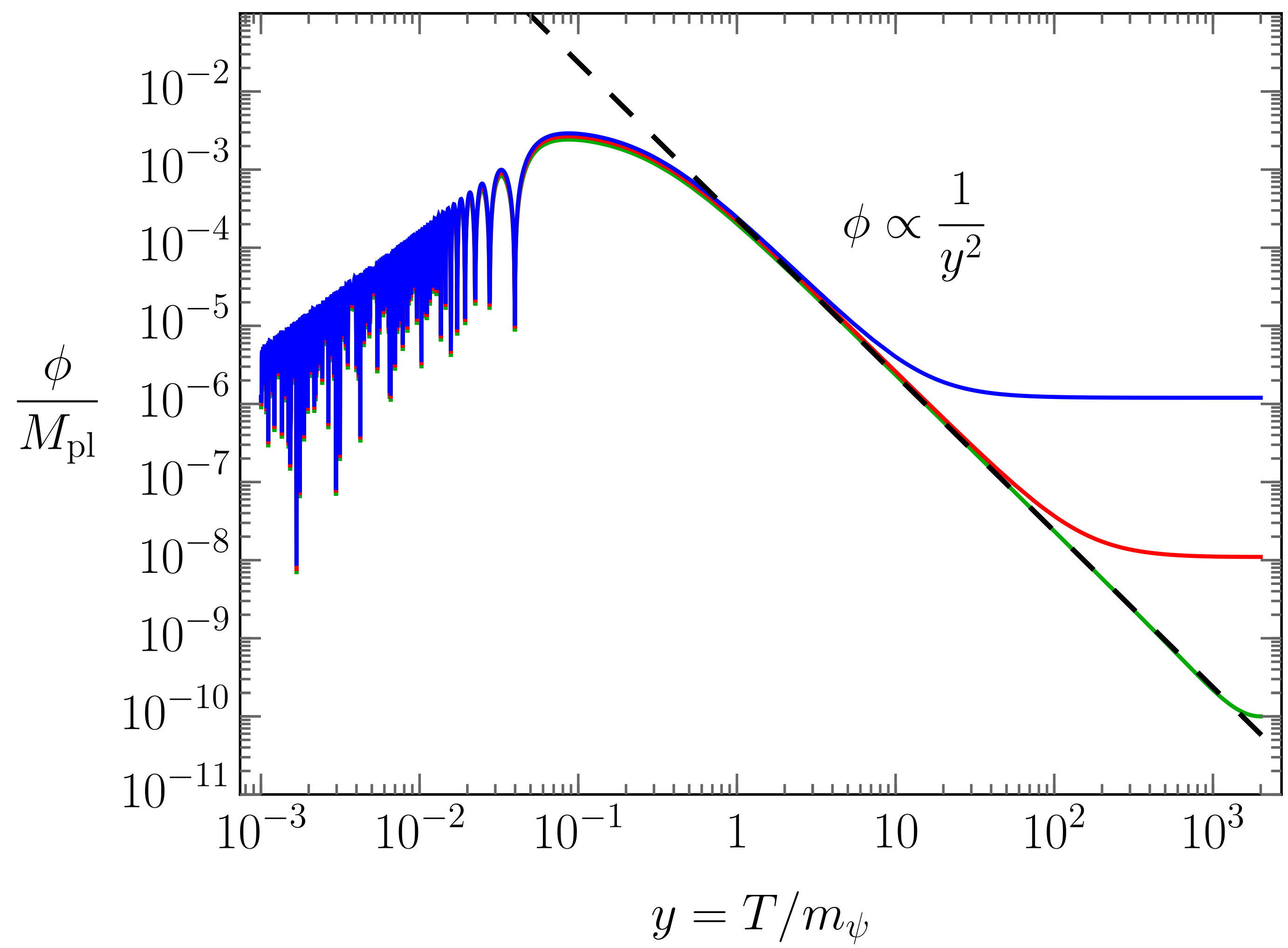

- For $\phi_i \ll M_{\text{pl}}/\beta$, the trajectory is not sensitive to the initial conditions

Onset of scalar oscillations

- The onset of oscillations occurs when the effective temperature-dependent scalar mass is equal to the Hubble rate. For $T_{\rm osc} \gg m_\psi$,

$$m_\phi^2(T) = m_\phi^2 + \frac{\beta^2 m_\psi^2 T^2}{6M_{\rm pl}^2} = m_\phi^2\left(1+\frac{\beta^2\, y^2}{6\,\kappa^2}\right) \qquad H(T) = \sqrt{\frac{\pi^2}{90}g_*(T)}\frac{T^2}{M_{\rm pl}} = \gamma\frac{m_\phi y^2}{\kappa}$$

$$\left.\frac{(3H(T))^2}{m_\phi^2(T)}\right|_{T_{\rm osc}} = 1 \quad \Rightarrow \quad y_{\rm osc} = \frac{\beta}{6\sqrt{3}\gamma}\sqrt{\left(1+\sqrt{1+\frac{1296\gamma^2\kappa^2}{\beta^4}}\right)}$$

$$\simeq \begin{cases} \dfrac{\beta}{3\sqrt{6}\gamma} & \text{for} \quad \beta \gg 6\sqrt{\gamma}\sqrt{\kappa} \\[2ex] \sqrt{\dfrac{\kappa}{3\gamma}} & \text{for} \quad \beta \ll 6\sqrt{\gamma}\sqrt{\kappa}. \end{cases}$$

- For $T_{\rm osc} \ll m_\psi$, the bare mass dominates and $y_{\rm osc} \simeq \sqrt{\kappa/3\gamma}$
- This suggests there are three qualitatively distinct regions of $\kappa - \beta$ parameter space.
- The boundaries of these regions are defined by the lines $y_{\rm osc} = 1$ and $\beta = 6\sqrt{\gamma}\sqrt{\kappa}$

Parameter space

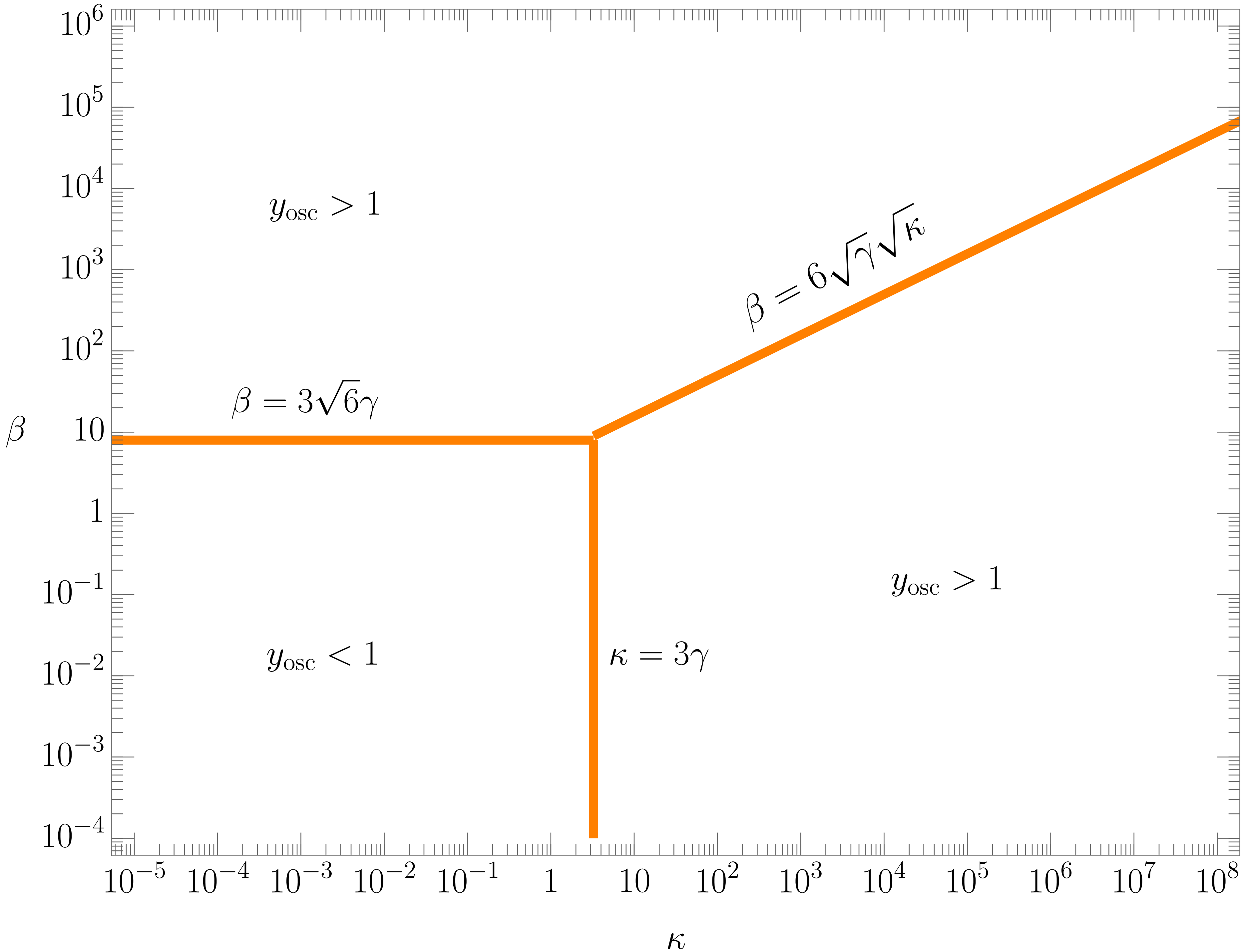

Region I (small β large κ, $y_{\rm osc} \gg 1$)

- This region is defined by $y_{\rm osc} > 1$ and $\beta < 6\sqrt{\gamma}\sqrt{\kappa}$, which implies $\kappa > 3\gamma$
- Initial trajectory: $\phi(y) \simeq \frac{\beta M_{\rm pl}}{36\gamma^2}\frac{1}{y^2}$
- As temperature decreases, scalar field grows until the onset of oscillations $y_{\rm osc} \simeq \sqrt{\frac{\kappa}{3\gamma}}$
- Oscillation amplitude $\phi_{\rm osc} \equiv \phi(y_{\rm osc}) \simeq \frac{\beta M_{\rm pl}}{12\gamma\kappa}$
- The scalar oscillates and redshifts as matter

$$\Omega_\phi\big|_0 = \frac{\rho_{\phi,0}}{\rho_{c,0}} = \frac{\frac{1}{2}m_\phi^2\phi_{\rm osc}^2(y_0/y_{\rm osc})^3(g_{*S}^0/g_{*S}^{\rm osc})}{\rho_{c,0}}$$

$$\simeq 2.2\times 10^5\left(\frac{m_\psi}{0.1\,{\rm GeV}}\right)\frac{\beta^2}{\kappa^{3/2}}$$

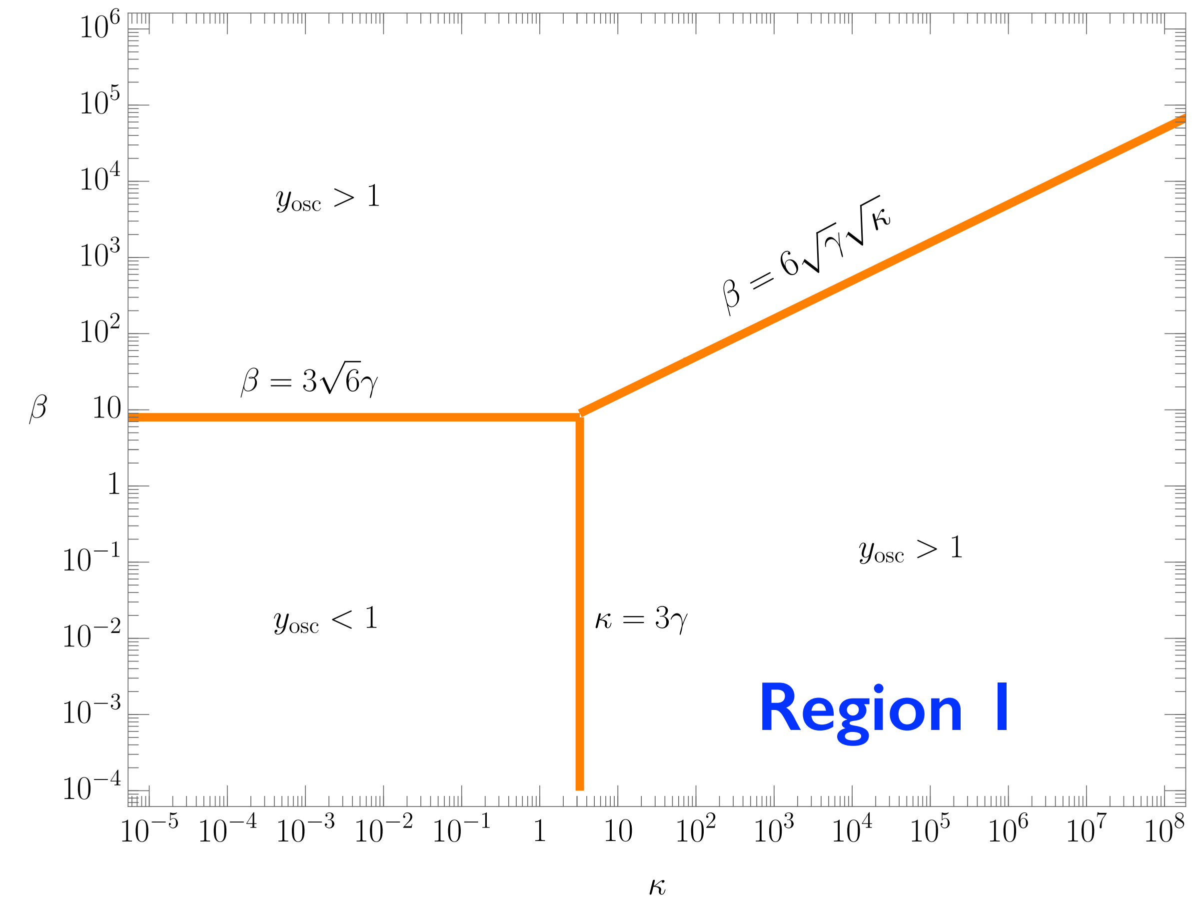

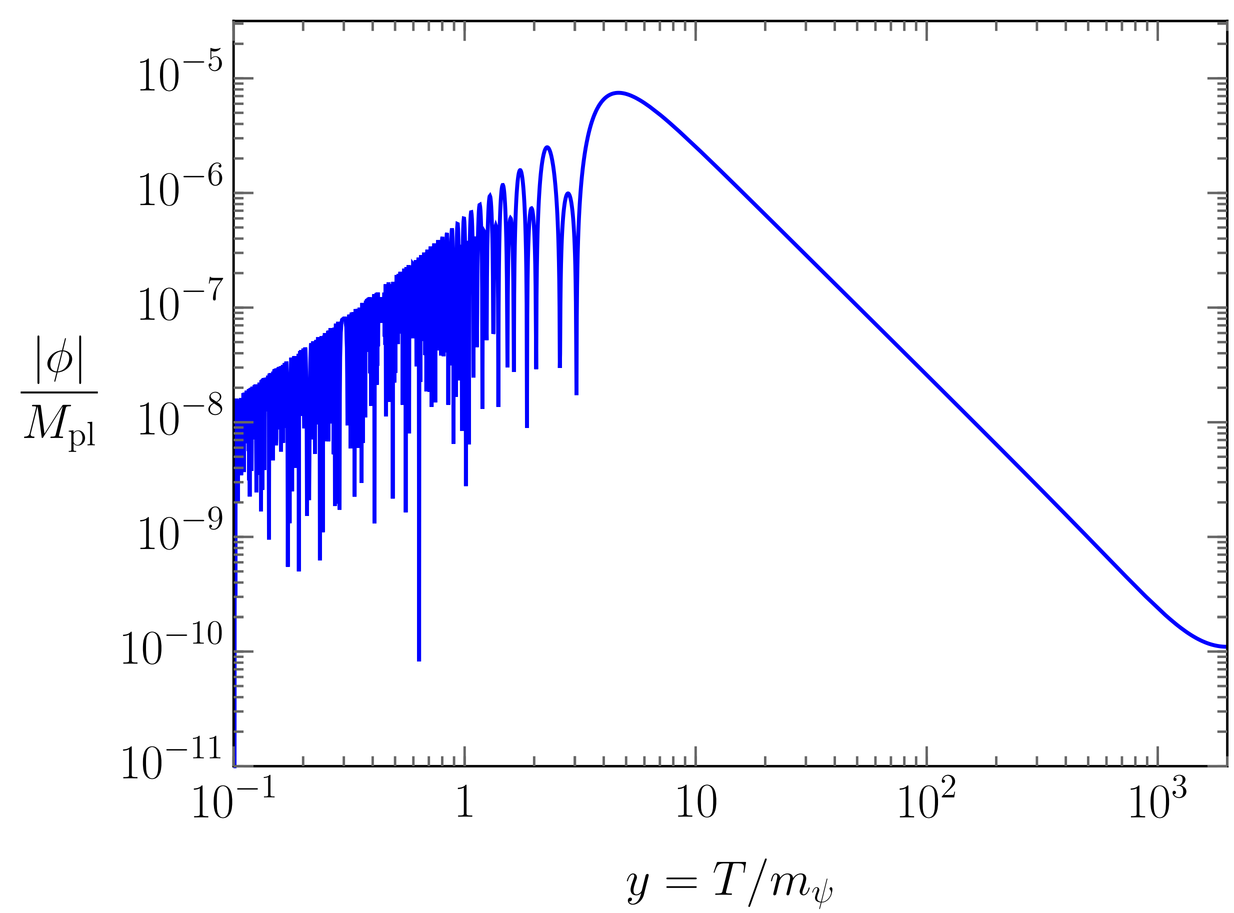

Region I relic density

$$\Omega_\phi\big|_0 \approx 0.3 \left(\frac{m_\psi}{0.1\,\mathrm{GeV}}\right)\left(\frac{\beta}{0.1}\right)^2\left(\frac{400}{\kappa}\right)^{3/2}$$

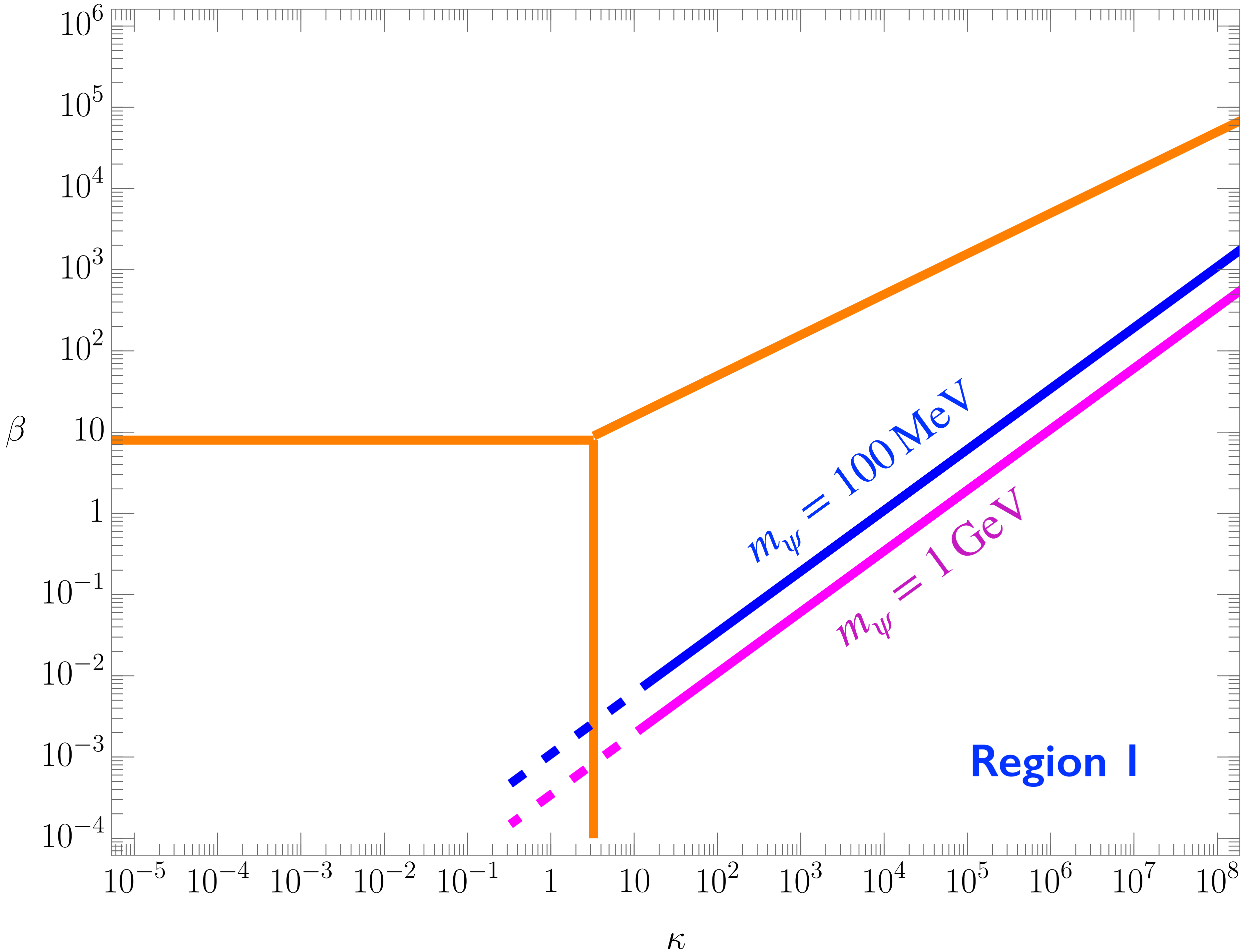

Region 2 (small β, small κ, $y_{\rm osc} \ll 1$)

- This region is defined by $y_{\rm osc} < 1$, implying both $\beta < 3\sqrt{6}\gamma$ and $\kappa < 3\gamma$

- Initial trajectory: $\phi(y) \simeq \dfrac{\beta M_{\rm pl}}{36\gamma^2}\dfrac{1}{y^2}$

- At $y \sim 1$, fermion is Boltzmann suppressed and the slope vanishes. The trajectory asymptotes to a maximum value, which is also the oscillation amplitude:

$$\phi_{\rm osc} \simeq 0.27\frac{\beta M_{\rm pl}}{\gamma^2} \qquad y_{\rm osc} \simeq \sqrt{\frac{\kappa}{3\gamma}}$$

- The scalar oscillates and redshifts as matter

$$\Omega_\phi\big|_0 = \frac{\rho_{\phi,0}}{\rho_{c,0}} = \frac{\frac{1}{2}m_\phi^2\phi_{\rm osc}^2(y_0/y_{\rm osc})^3(g_{*S}^0/g_{*S}^{\rm osc})}{\rho_{c,0}}$$

$$\simeq 2.3\times 10^6\left(\frac{m_\psi}{0.1\,{\rm GeV}}\right)\beta^2\sqrt{\kappa}$$

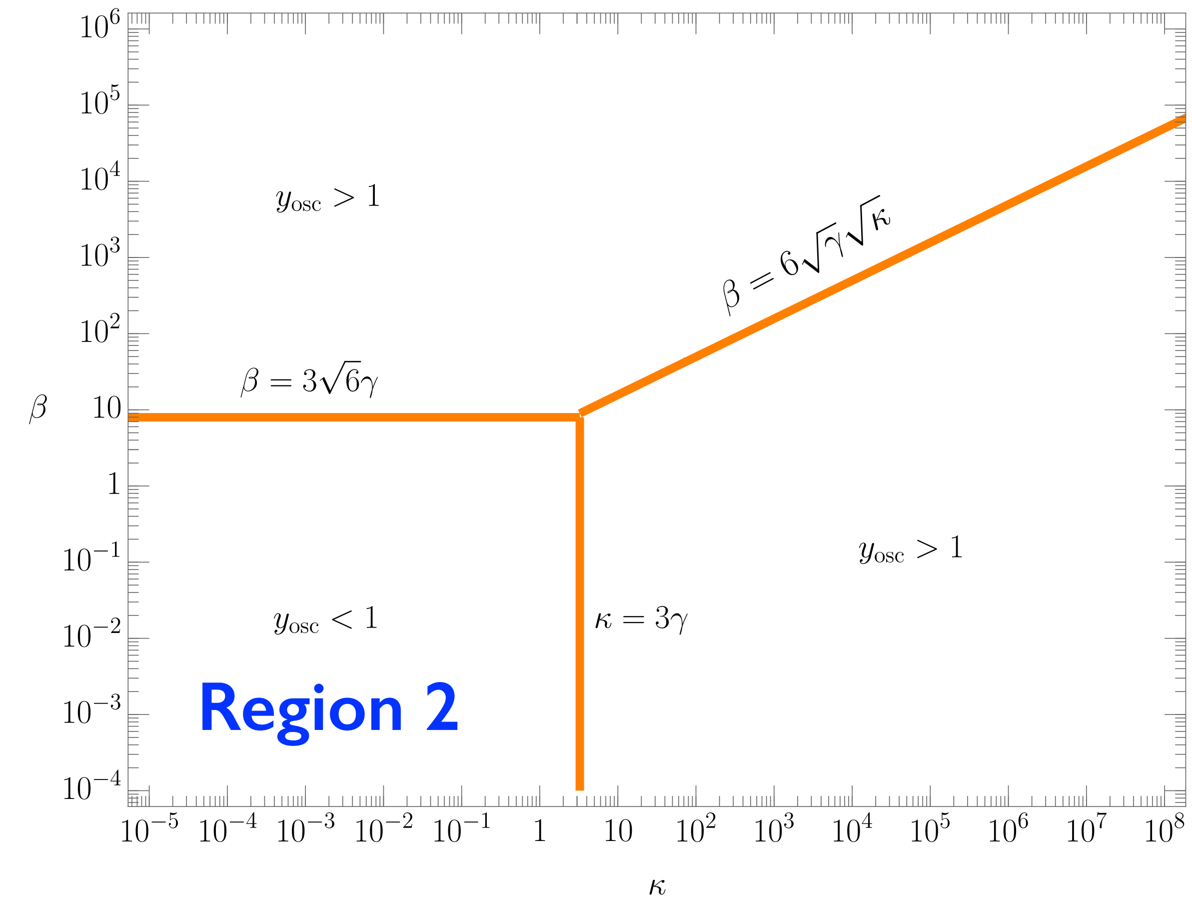

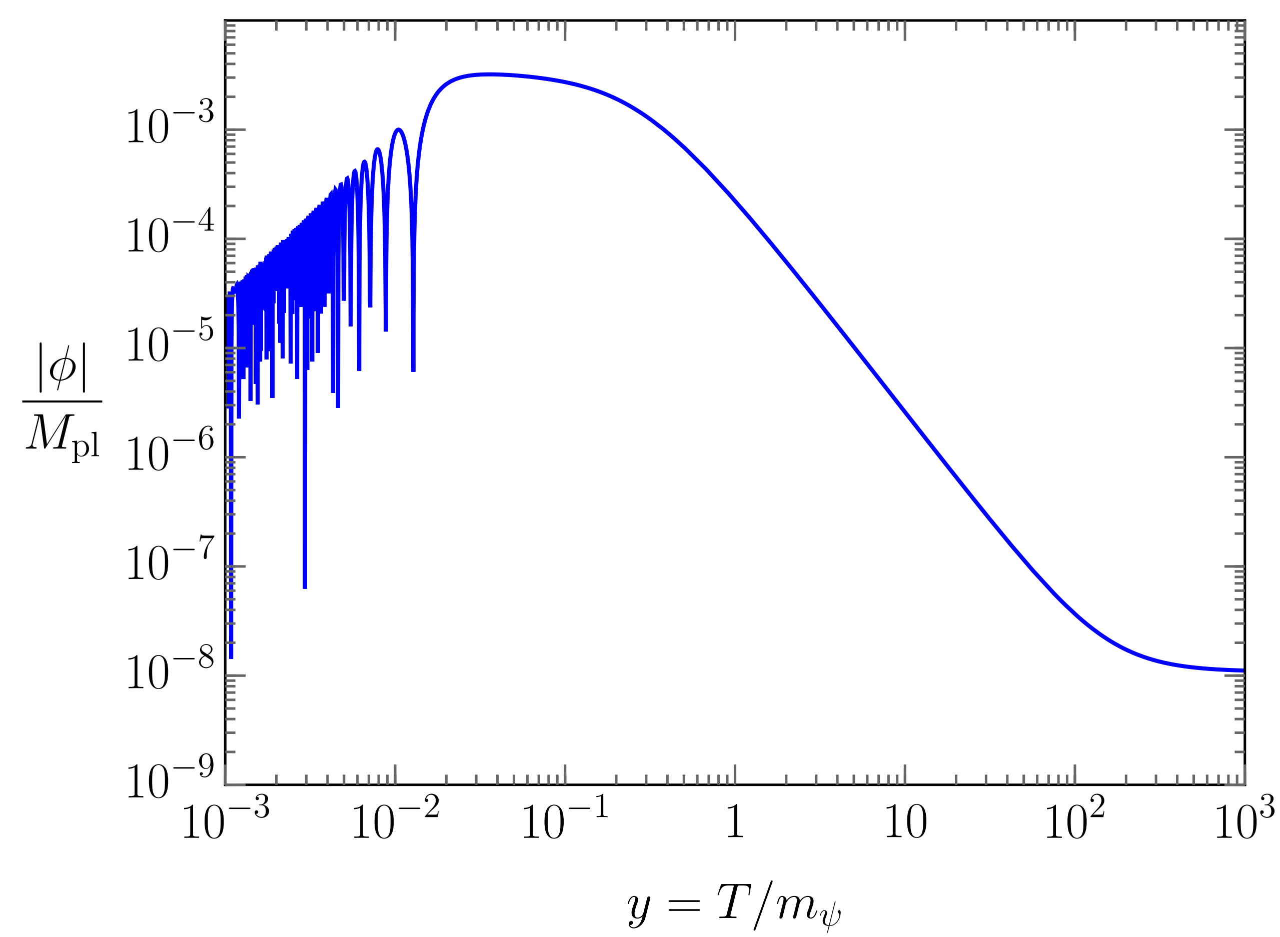

Region 2 relic density

$$\Omega_\phi\big|_0 \approx 0.3 \left(\frac{m_\psi}{0.1\,\mathrm{GeV}}\right)\left(\frac{\beta}{10^{-3}}\right)^2\left(\frac{\kappa}{0.02}\right)^{1/2}$$

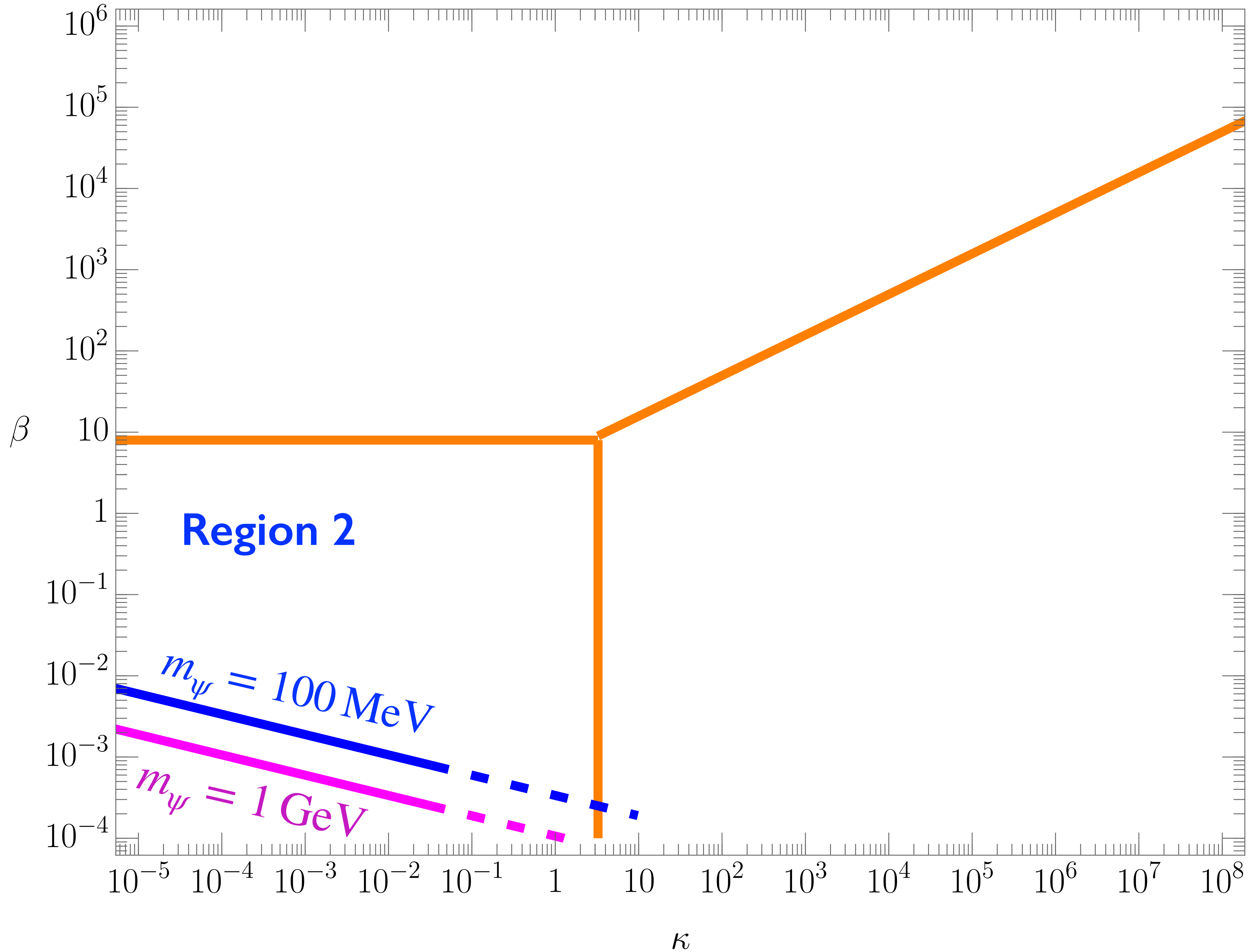

Regions 1 & 2 Relic Density

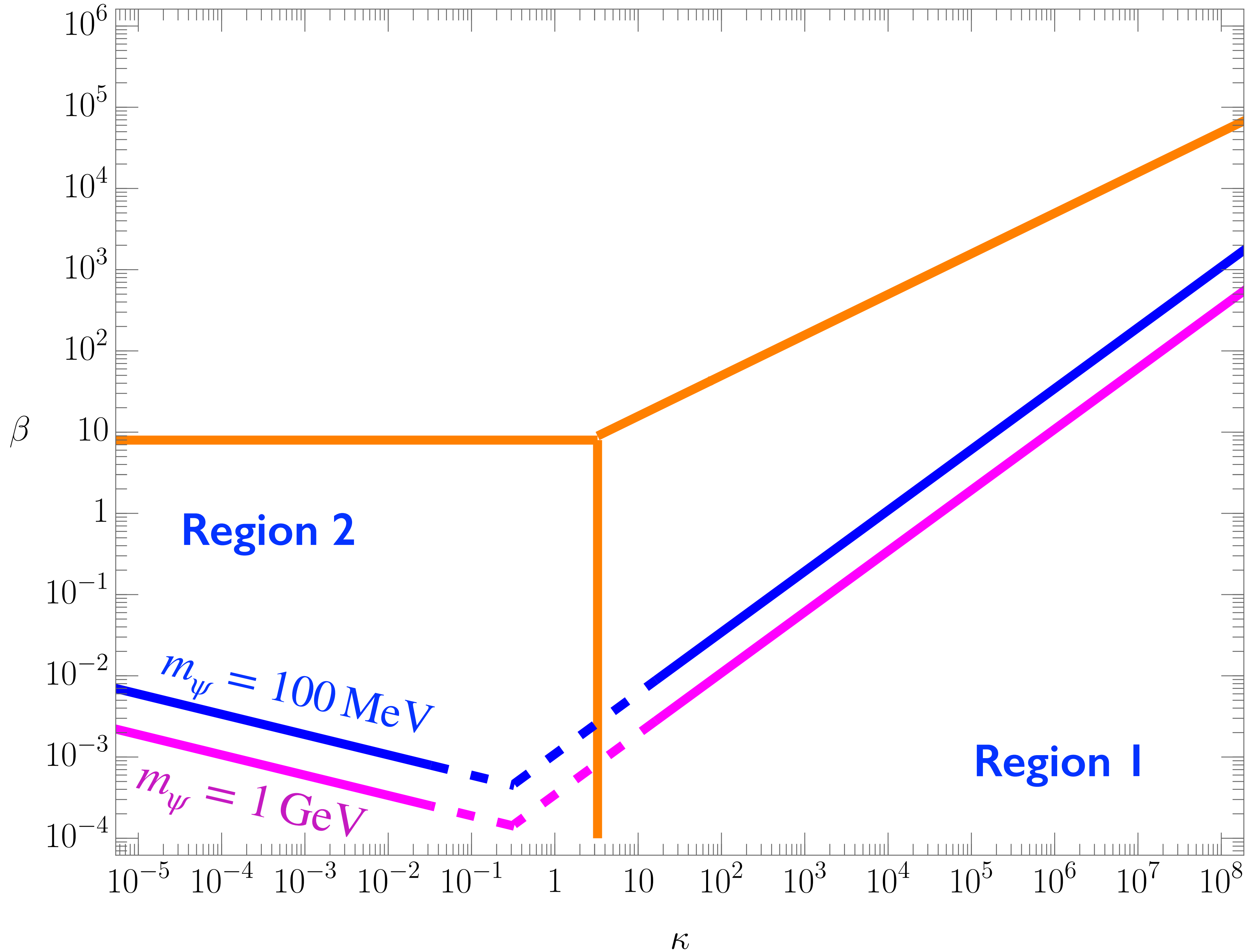

Regions 1 & 2 Relic Density

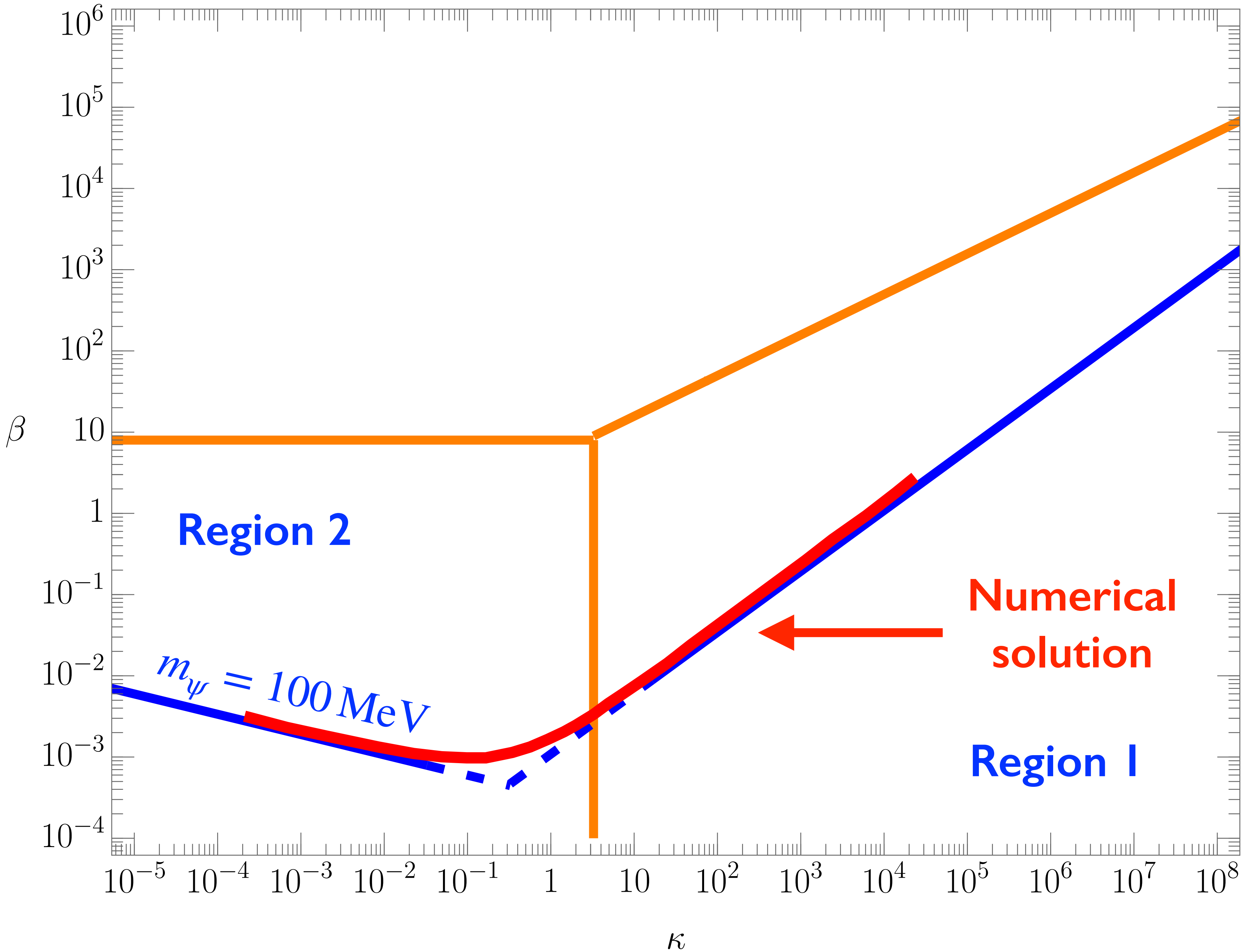

Initial conditions and inflation

- During inflation, the evolution of the DM scalar field involves a competition between classical rolling and quantum fluctuations

- Given a long enough period of inflation with order $N_e \sim H_I^2/m_\phi^2$ e- folds, the distribution of the scalar approaches a Gaussian with mean close to zero and variance $\sigma_\phi \sim H_I^4/m_\phi^2$.

- We require two conditions to be met:

  1. $\sigma_\phi \ll \phi_{\rm osc}$ in order to avoid fine tuning of initial conditions
  2. The reheat temperature to be greater than the oscillation temperature.

- It can be shown that these two conditions can always be satisfied for a suitable range of values for the Hubble parameter during inflation. This typically requires a low Hubble scale and long period of inflation.

- A low Hubble scale during inflation also suppresses the primordial scalar DM fluctuations, thereby evading otherwise stringent isocurvature constraints

Realistic example: scalar DM coupled to muon

$$-\mathcal{L} \supset \frac{1}{2} m_\phi^2 \phi^2 + m_\mu \left(1 - \frac{\beta \phi}{M_{\rm pl}}\right) \bar{\mu} \mu$$

- The required coupling is obtained from the dimension-5 operator

$$\mathcal{L} \supset \frac{c_\ell}{M_{\rm pl}} \phi \, \overline{L}_L \, \ell_R \, H + \text{h.c.} \qquad c_\ell = \frac{\sqrt{2}\, m_\ell}{v} \beta = y_\ell \, \beta$$

- At temperatures above the electroweak scale, the fermion feedback turns off (fermion is massless). Fermion feedback turns on at $T \lesssim v_{\rm EW}$

- The scalar potential is fine-tuned when $\delta m_\phi^2 \sim \dfrac{\beta^2 m_\mu^2 v^2}{16\pi^2 M_{\rm pl^2}} \gtrsim m_\phi^2$

- The previous results for the relic density prediction can be applied by fixing the fermion mass to the muon mass

Relic density

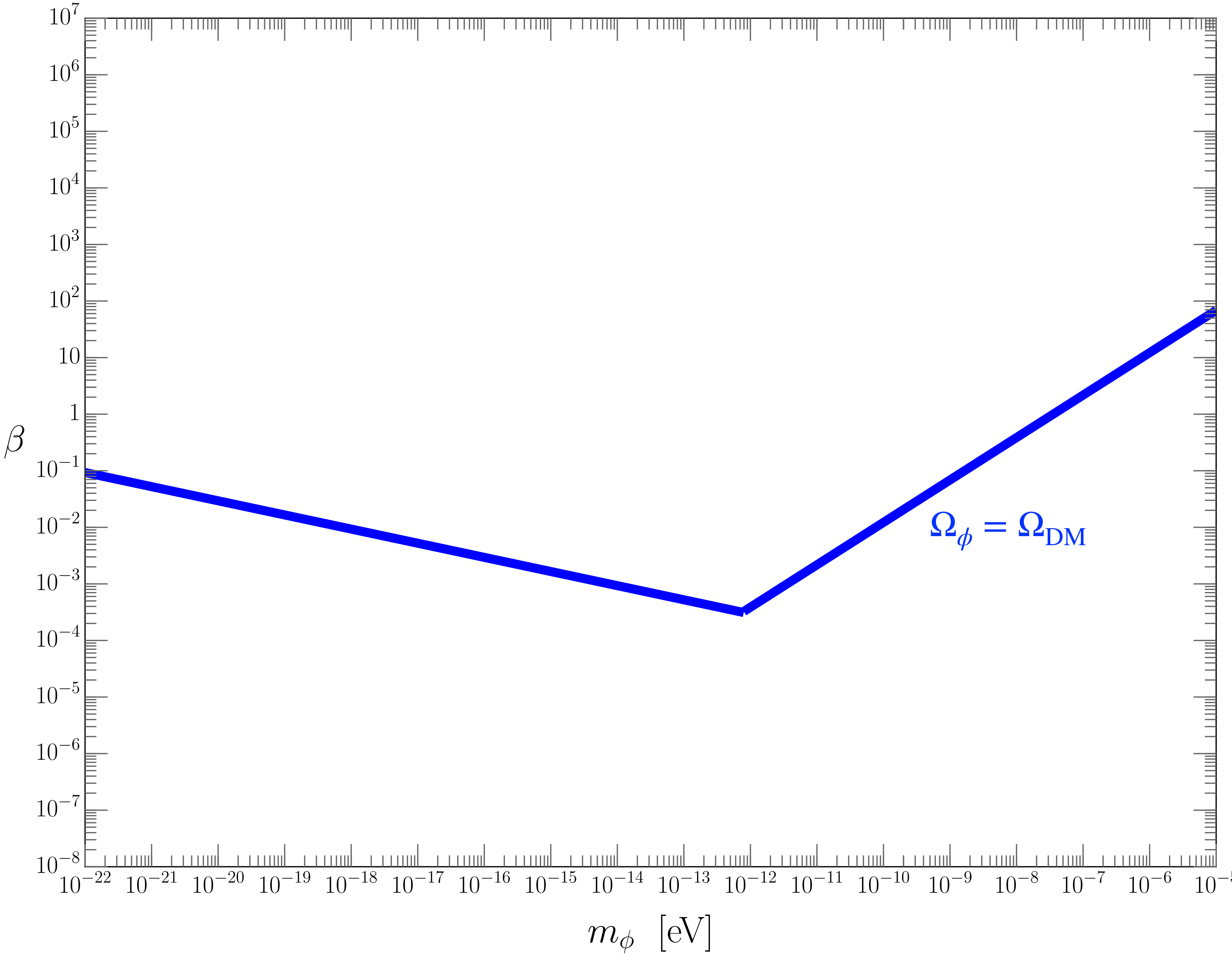

Naturalness

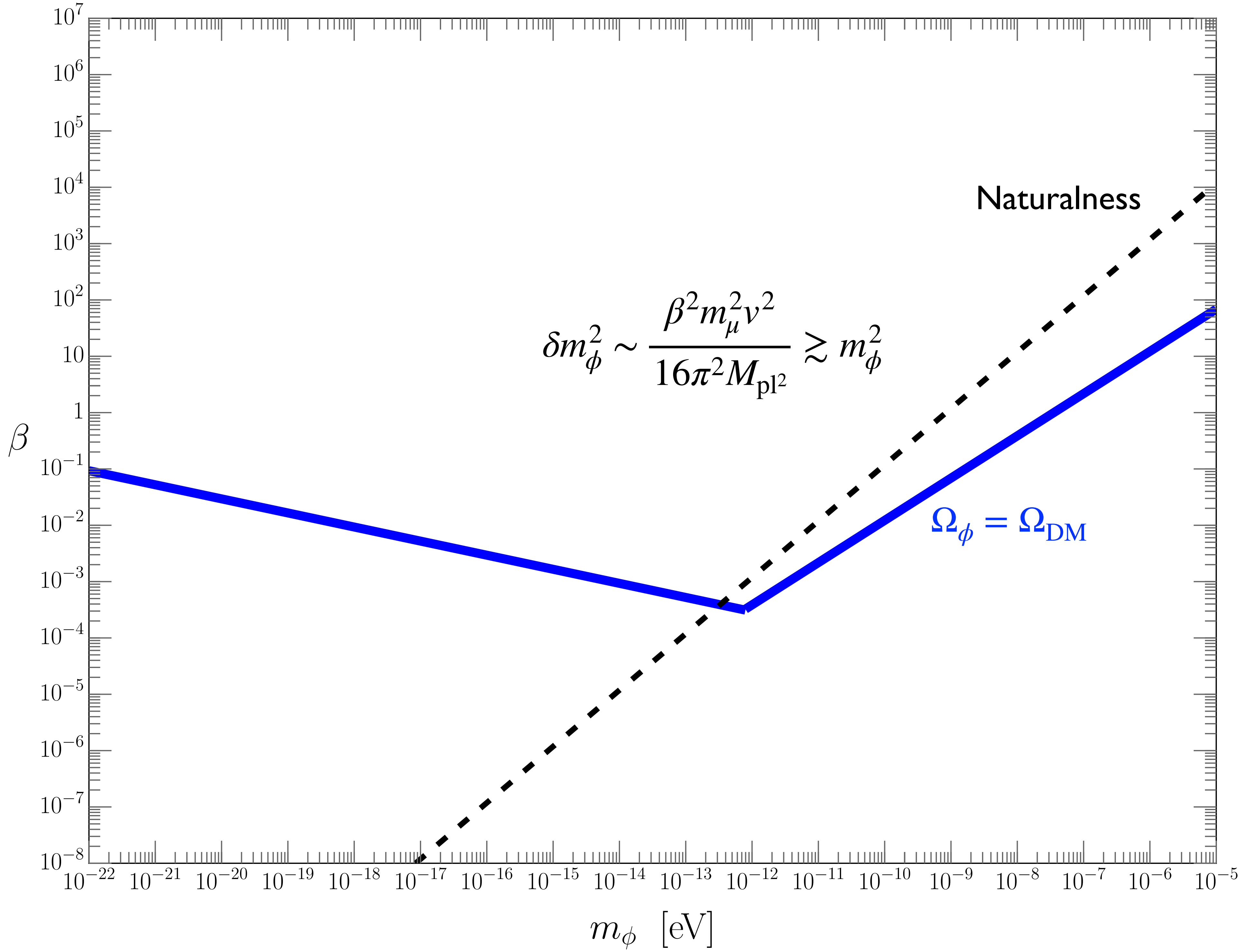

Experimental/observational probes

Lyman-α / Fuzzy DM constraints

- In the Fuzzy DM regime (De Broglie wavelength of ~ 1 kpc), matter power at small scales is suppressed

- The Lyman-alpha forest flux power spectrum provides a tracer of matter fluctuations on small scales and high-redshifts (quasi-linear regime)

- Lyman-alpha constrains DM masses $m_\phi > 2 \times 10^{-21}\,\mathrm{eV}$

[Irsic, et al. '17]

- Only relies on gravitational interaction

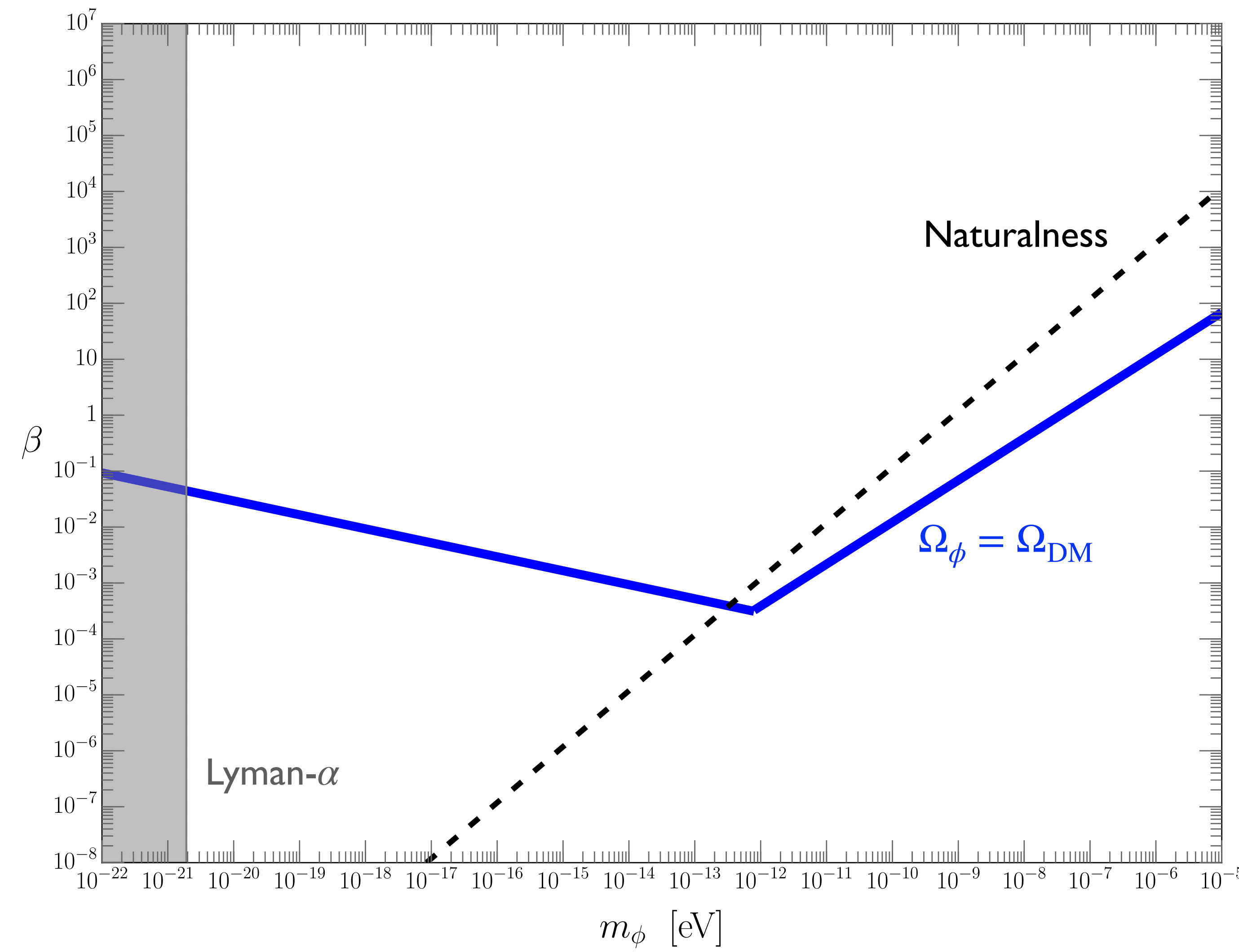

Black hole superradiance

- Light bosons with Compton wavelength of order size of spinning black hole will extract its angular momentum via the superradiance effect

- The observation of such spinning black holes therefore constrains such light bosons

- Superradiance provides strongest constraints for $m_\phi \sim 10^{-12}\,\mathrm{eV}$

[Baryakhtar, Galanis, Lasenby, Simon,'20]

- Only relies on gravitational interaction

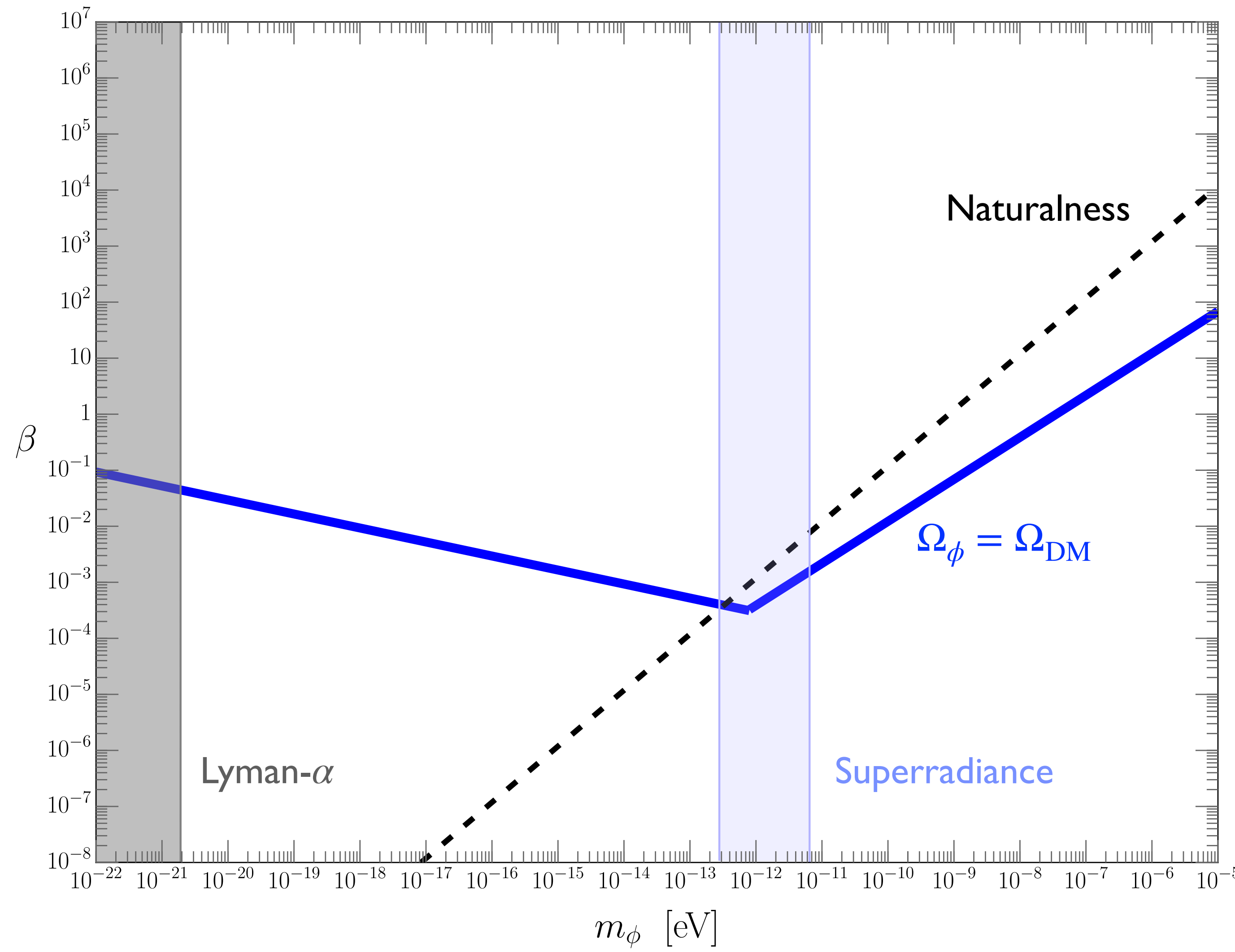

Muon storage ring tests and $(g-2)_\mu$

[Janish, Ramani, '20]

- DM coupled to muons will induce an oscillating muon mass and thus alter the muon precession frequency in storage ring experiments (e.g., BNL and FNAL muon $g-2$)

$$\omega_a = -a_\mu \frac{e\vec{B}}{m_\mu} \quad \Rightarrow \quad \vec{\omega}_{dm} = \vec{\omega}_{sm} \frac{\lambda}{m_\mu} \frac{\sqrt{2\rho_\phi}}{m_\phi} \cos(m_\phi t)$$

- BNL experiment constrains small DM masses, large couplings
- A time-resolved analysis could provide stronger constraints
- Directly probes DM coupling to muon

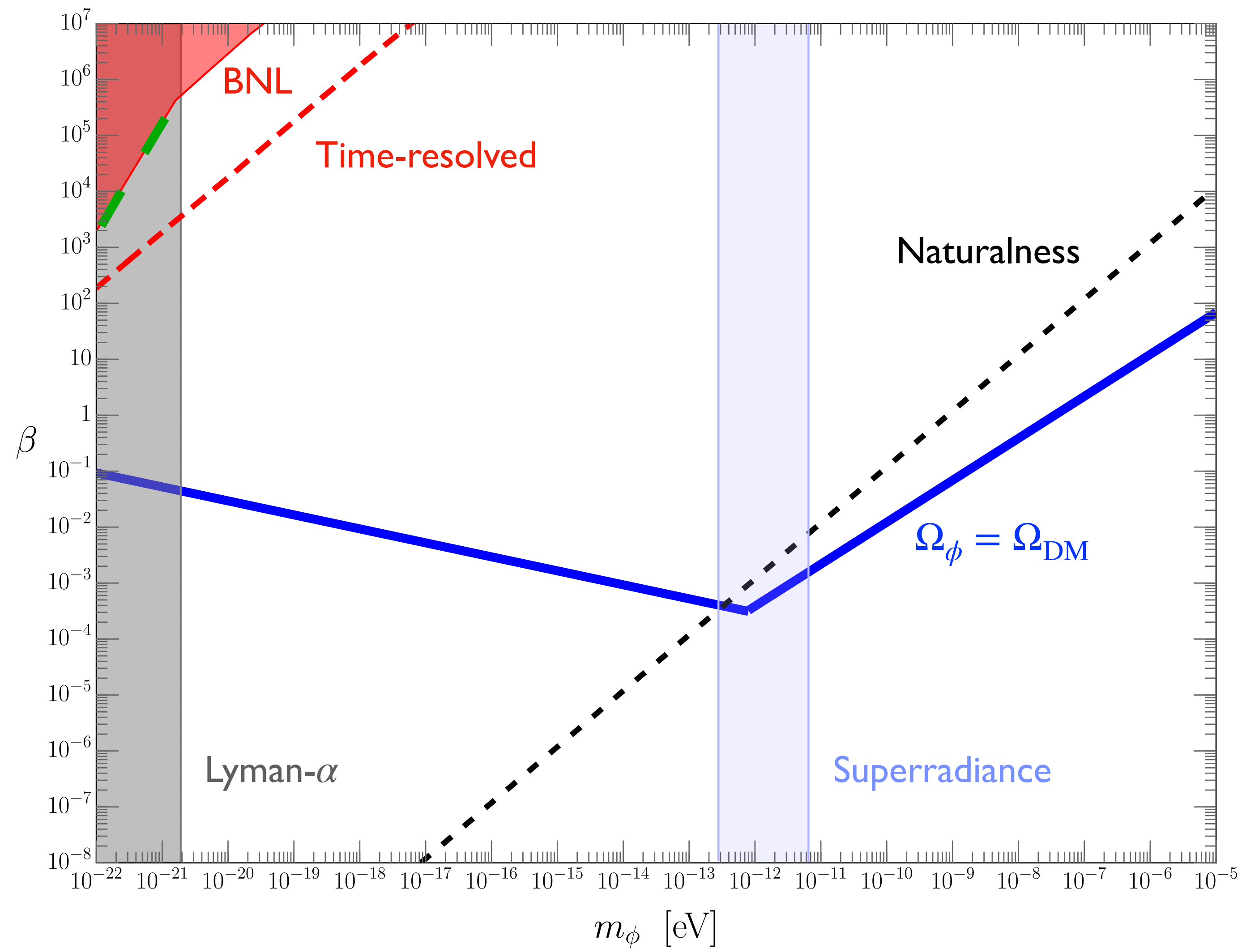

Muonic forces in neutron star binaries

[Dror, Laha, Opferkuch '20]

- Neutron stars (NS) are muon-rich environments. The properties of NS binaries can therefore be modified if there is a long-range muonic force

- Pulsar binaries will exhibit anomalously fast decay of their orbital period due to emission of the muonic force carriers

- The additional long range force between merging NS-NS binaries modifies the inspiral phase and resulting pattern of gravitational radiation

- Probes DM coupling to muon

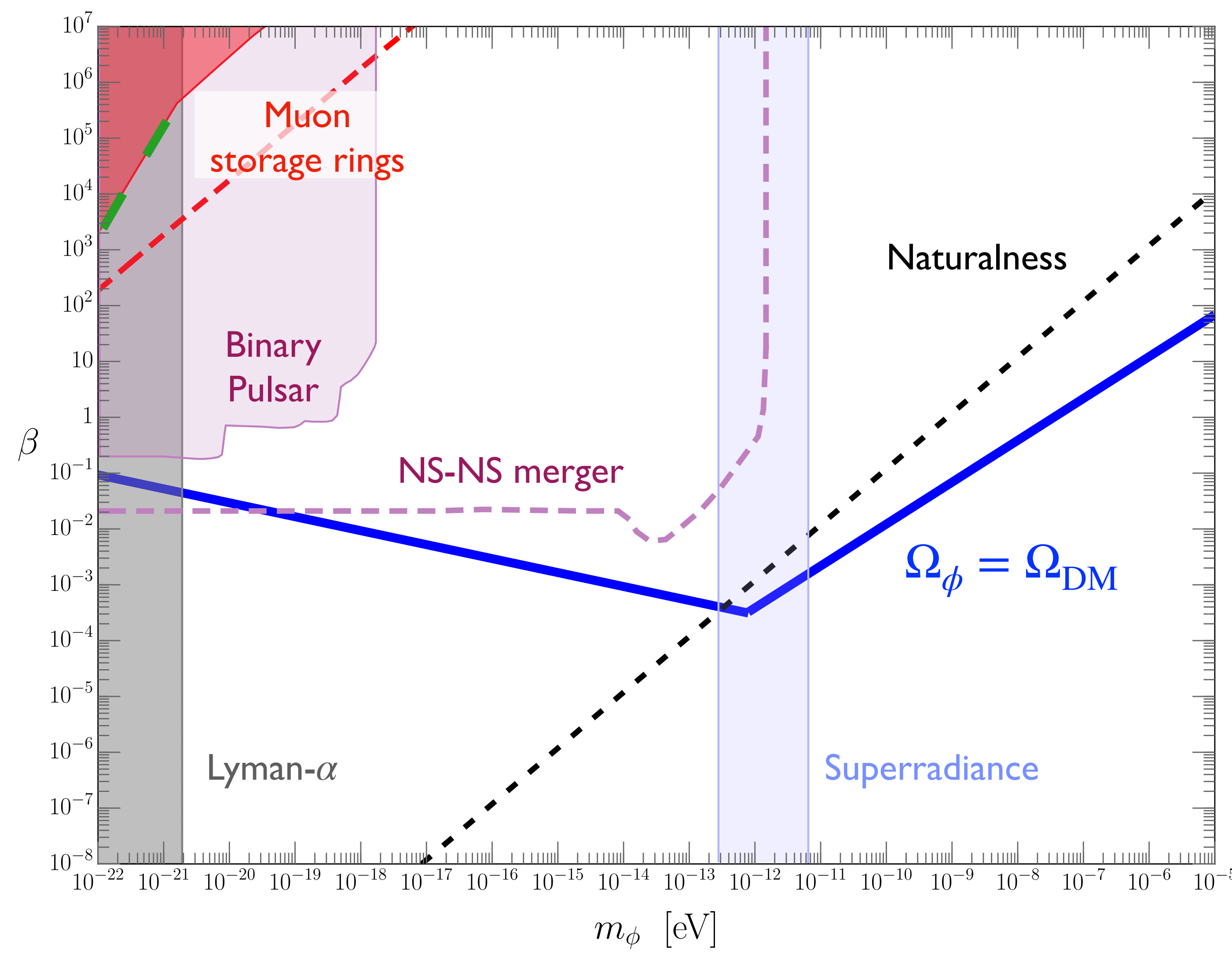

Equivalence principle & inverse square law tests

- At one (two) loop(s), DM can couple to photons (charged fermions)

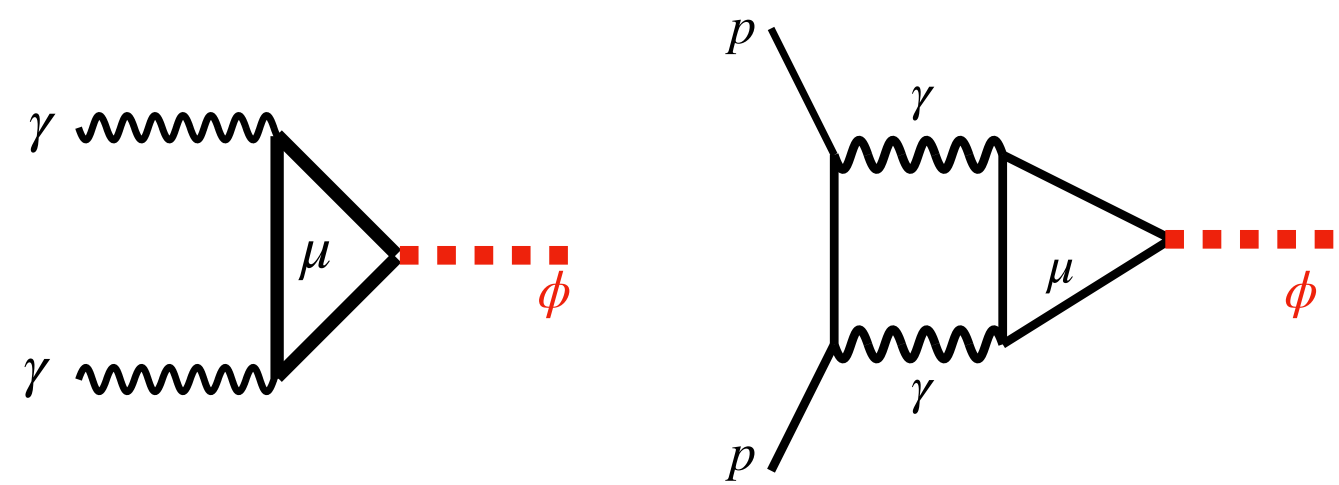

- This induces a long range Yukawa force, which can be probed by equivalence principle and inverse square law tests

  [Schlamminger et al. , '07]
  [Wagner et al. , '12]

- Indirect probe of the DM-muon coupling

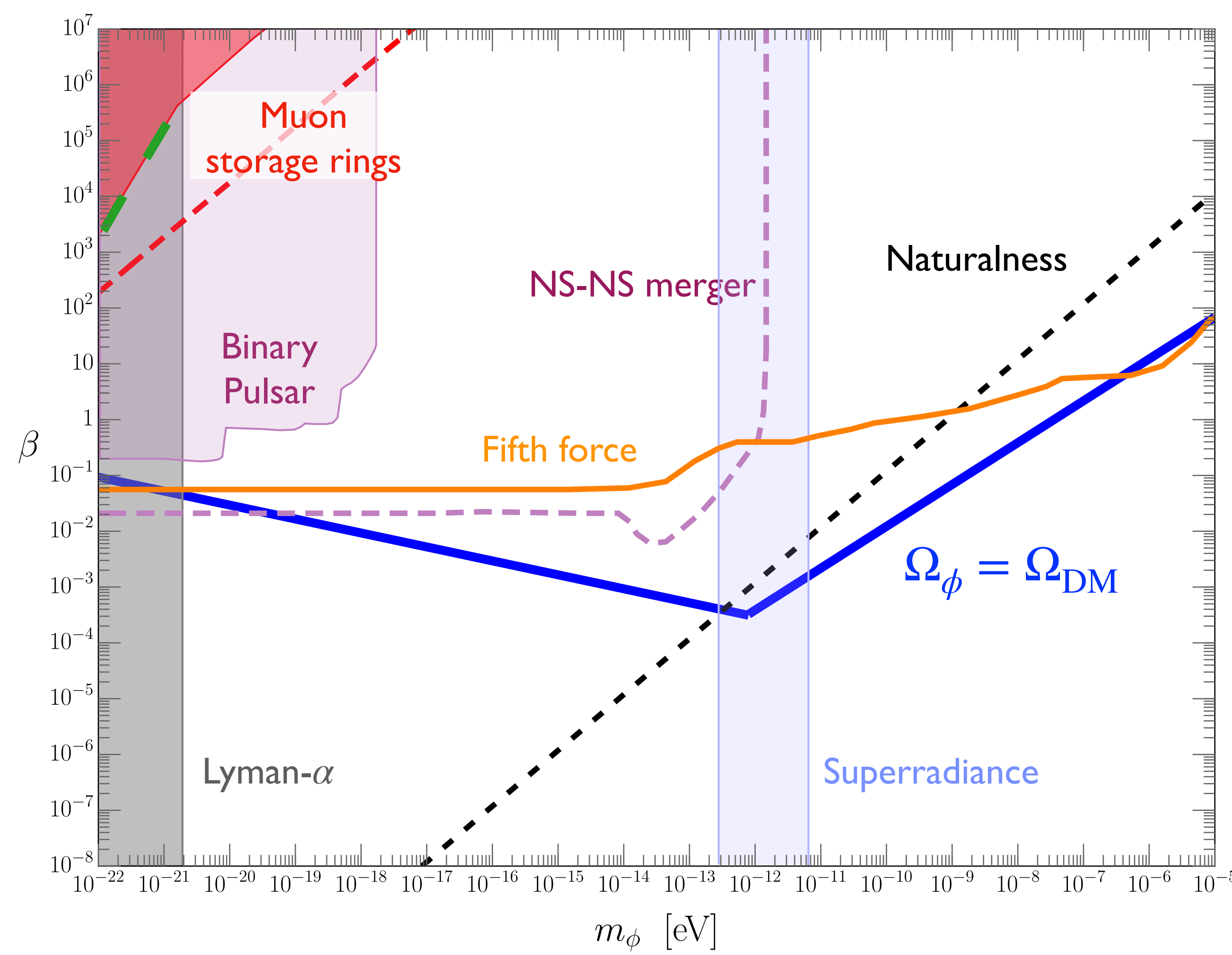

Variation in fine structure constant

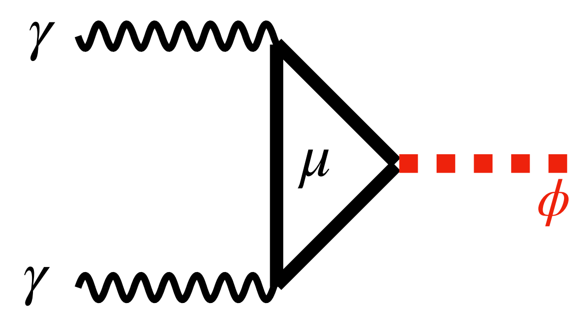

- At one loop the DM can couple to photons
- This leads to temporal variations of the fine structure constant in the dark matter background
- Strong existing limits come atomic clocks measurements (e.g. Rb/Cs hyper fine transition frequency ratio)

  [Hees et al. '16]

- Future atom interferometry experiments can cover substantial new parameter space

  [Arvanitaki et al. 16]

- Indirect probe of the DM-muon coupling

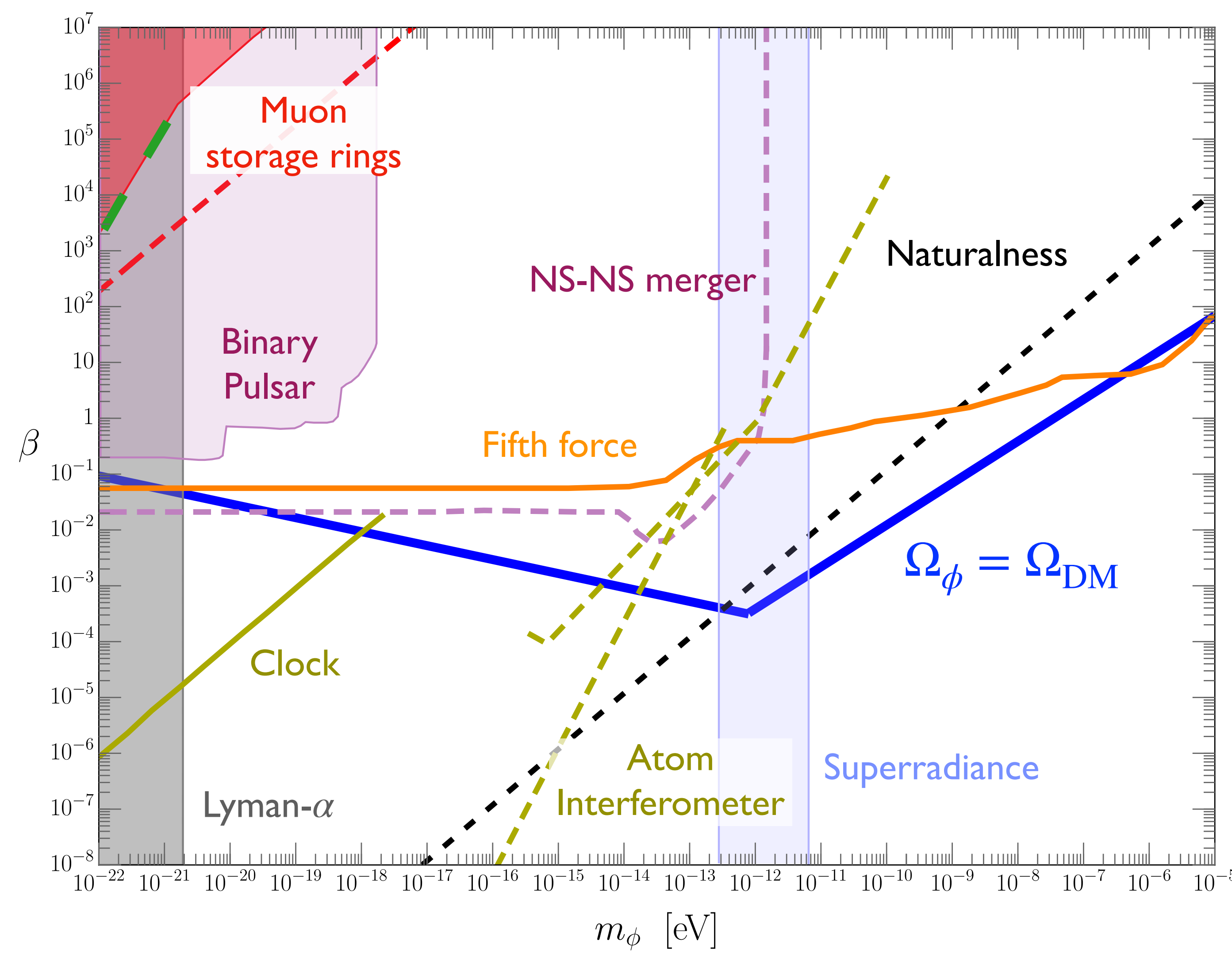

Summary

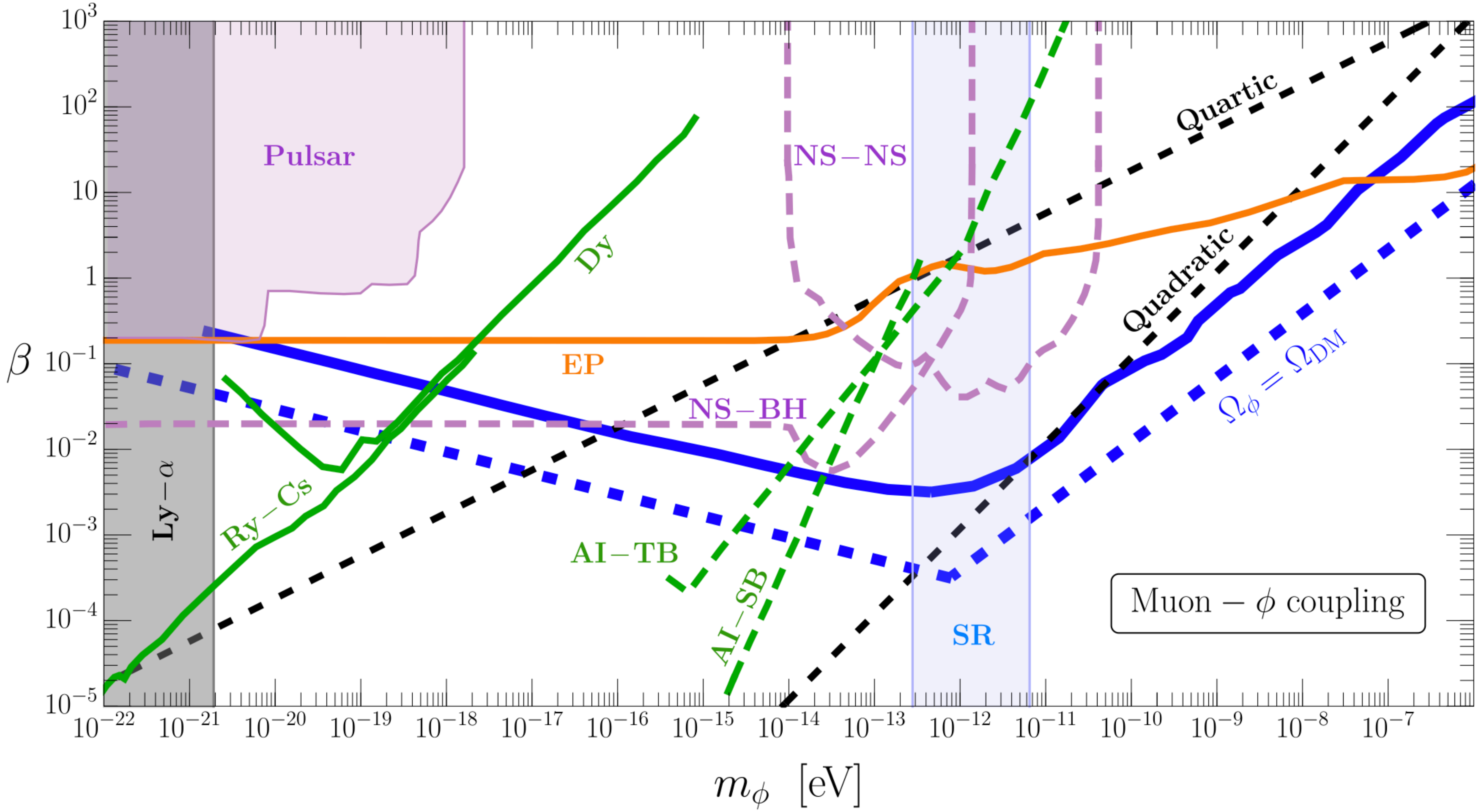

Pulsar
Dy
NS−NS
Quartic
Quadratic
EP
NS−BH
Ry−Cs
Ly−α
AI−TB
AI−SB
SR
$\Omega_\phi = \Omega_{DM}$
Muon − ϕ coupling
β
m_ϕ [eV]
10^3
10^2
10
1
10^{-1}
10^{-2}
10^{-3}
10^{-4}
10^{-5}
10^{-22} 10^{-21} 10^{-20} 10^{-19} 10^{-18} 10^{-17} 10^{-16} 10^{-15} 10^{-14} 10^{-13} 10^{-12} 10^{-11} 10^{-10} 10^{-9} 10^{-8} 10^{-7}

Outlook

- Ultralight bosons represent a well-motivated and phenomenologically distinctive class of DM models

- We have presented *thermal misalignment* — a mechanism to dynamically generate the large misalignment needed to obtain the correct DM relic abundance

- The mechanism relies on a finite temperature potential due to a coupling of DM to a fermion. It is insensitive to initial conditions and the abundance is dictated by the microphysics (couplings and masses)

- We have studied the phenomenology of a realistic scenario where the DM couples to the muon. A variety of opportunities for probing this scenario in the future exist.

- In progress/future work: couplings of DM to other fermions, couplings to bosons, Higgs portal as UV completion